

1 Paratransgenic manipulation of tsetse *miR275* alters the physiological homeostasis of the fly's
2 midgut environment

3 Liu Yang^a, Brian L. Weiss^a, Adeline E. Williams^{a,b}, Emre Aksoy^{a,c}, Alessandra de Silva Orfano^a, Jae
4 Hak Son^a, Yineng Wu^a, Aurelien Vigneron^{a,d}, Mehmet Karakus^{a,e}, Serap Aksoy^a

5 ^aDepartment of Epidemiology of Microbial Diseases, Yale School of Public Health, New Haven,
6 CT, United States of America

7 ^bDepartment of Microbiology, Immunology, Pathology, Colorado State University, Fort Collins,
8 CO, USA

9 ^cDepartment of Immunology and Infectious Diseases, Harvard T.H. Chan School of Public
10 Health, Boston, MA, USA

11 ^dDepartment of Evolutionary Ecology, Institute for Organismic and Molecular Evolution,
12 Johannes Gutenberg University, Mainz, Germany

13 ^eDepartment of Medical Microbiology, Faculty of Medicine, University of Health Sciences,
14 Istanbul, Turkey

15

16

17

18

20 **Abstract**

21 Tsetse flies are vectors of parasitic African trypanosomes (*Trypanosoma* spp.). Current disease
22 control methods include fly-repelling pesticides, trapping flies, and chemotherapeutic
23 treatment of infected people. Inhibiting tsetse's ability to transmit trypanosomes by
24 strengthening the fly's natural barriers can serve as an alternative approach to reduce disease.
25 The peritrophic matrix (PM) is a chitinous and proteinaceous barrier that lines tsetse's midgut.
26 It protects the epithelial cells from the gut lumen content such as food and invading
27 trypanosomes, which have to overcome this physical barrier to establish an infection.
28 Bloodstream form trypanosomes shed variant surface glycoproteins (VSG) into tsetse's gut
29 lumen early during the infection establishment. The VSG molecules are internalized by the fly's
30 PM-producing cardia, which results in a reduction in tsetse *miR275* expression and a sequential
31 molecular cascade that compromises the PM integrity. In the present study, we investigated
32 the role(s) of *miR275* in tsetse's midgut physiology and trypanosome infection processes by
33 developing a paratransgenic expression system. We used tsetse's facultative bacterial
34 endosymbiont *Sodalis glossinidius* to express tandem antagonir-275 repeats (or *miR275*
35 sponge) that constitutively reduce *miR275* transcript abundance. This paratransgenic system
36 successfully knocked down *miR275* levels in the fly's midgut, which consequently obstructed
37 blood digestion and modulated infection outcomes with an entomopathogenic bacteria and
38 with trypanosomes. RNA sequencing of cardia and midgut tissues from the paratransgenic
39 tsetse confirmed that *miR275* regulates processes related to the expression of PM-associated
40 proteins and digestive enzymes as well as genes that encode abundant secretory proteins. Our

- 41 study demonstrates that paratransgenesis can be employed to study microRNA- regulated
- 42 pathways in arthropods housing symbiotic bacteria.

44 **Author Summary**

45 Tsetse flies transmit African trypanosomes, which are the parasites that cause sleeping sickness
46 in human in sub-Saharan Africa. When tsetse ingests a blood meal containing trypanosomes,
47 the expression level of a microRNA (*miR275*) decreases in the fly's gut. This process results in a
48 series of events that interrupt the physiological homeostasis of the gut environment. To further
49 understand the function of *miR275* in tsetse fly, we genetically modified a tsetse's native
50 bacterial symbiont, reintroduced the genetically modified bacterium back into the fly, and
51 successfully knocked down the *miR275* expression in tsetse's midgut. These 'paratransgenic'
52 flies (which house genetically modified bacteria) presented impaired digestive processes and
53 were highly susceptible to infection with trypanosomes. Lastly, we discovered that *miR275*
54 regulates tsetse secretory pathways. Our novel paratransgenic expression system can be
55 applied to study the function of other microRNAs and how they regulate disease transmission
56 in tsetse and other insect systems.

57

58 **1. Introduction**

59 Tsetse flies (*Glossina* spp.) are obligate vectors of pathogenic African trypanosomes
60 (*Trypanosoma* spp.) throughout 37 countries in sub-Saharan Africa (1). These protozoan
61 parasites cause human and animal African trypanosomiases (HAT and AAT, respectively), both
62 of which are fatal if left untreated (2, 3). Current disease control methods include vector control
63 to reduce population size and chemotherapeutic treatment of infected people and
64 domesticated animals (4). A more complete molecular understanding of tsetse-trypanosome
65 interactions will facilitate the development of novel control strategies, such as reducing or
66 eliminating the fly's capacity to transmit trypanosomes.

67 The tsetse-specific stages of the trypanosome life cycle begin when the fly ingests a
68 bloodmeal that contains mammalian stage bloodstream form (BSF) parasites. Upon ingestion
69 by tsetse, BSF parasites differentiate into insect adapted procyclic forms (PCF) in the lumen of
70 the fly's midgut (5, 6). PCF parasites then bypass the fly's peritrophic matrix (PM) barrier in the
71 anterior midgut and replicate within the ectoperitrophic space (ES, the region between the PM
72 and the midgut epithelia) (7-9). As part of their development from BSF to PCF parasites, the BSF
73 trypanosomes shed their abundant surface coat antigens, known as variant surface
74 glycoprotein (VSG) into the fly's midgut lumen. Free VSG is transiently internalized by cells of
75 tsetse's PM-producing cardia (also known as proventriculus) (10, 11). This process reduces the
76 expression of genes that encode PM associated proteins and digestive enzymes, and modulates
77 the expression of several microRNAs, including a drastic reduction in the expression of tsetse
78 *microRNA 275 (miR275)* (11).

79 miRNAs are small (~23 nucleotides) non-coding RNAs that regulate many important
80 physiological processes. miRNAs often suppress gene expression by guiding the Argonaute
81 (AGO) protein to bind with its target mRNA, which induces the miRNA induced silencing
82 complex (miRISC) and leads to post-transcriptional repression or degradation of the target
83 mRNA (12-14). miRNAs can also upregulate gene expression by inducing translational activation
84 (15, 16). When the expression of *miR275* was experimentally reduced in tsetse's cardia and
85 midgut through the provisioning of synthetic anti-*miR275* antagonirs (antagomir-275) or VSG
86 purified from BSF trypanosomes, formation of the fly's PM was impaired. This process disrupted
87 blood meal digestion and enhanced the ability of trypanosomes to establish an infection in the
88 fly's midgut (11). In the mosquito *Aedes aegypti*, *miR275* similarly influences midgut blood
89 digestion and fluid excretion by regulating the expression of its target gene *SERCA*
90 (sarco/endoplasmic reticulum Ca²⁺ adenosine triphosphatase) (17, 18) but the mRNA target of
91 *miR275* in tsetse remains unknown.

92 Tsetse flies house a consortium of symbiotic microbes that mediate numerous aspects
93 of their host's physiology (19, 20). One of these is the facultative endosymbiotic bacterium
94 *Sodalis glossinidius*, which resides extra- and intracellularly within multiple tsetse tissues,
95 including the midgut, salivary glands, and reproductive organs (21). *Sodalis* can be cultivated
96 and genetically modified *in vitro*, and recolonized into tsetse's gut via a blood meal (22, 23).
97 Reintroducing recombinant *Sodalis* (rec*Sodalis*) does not elicit immune responses that would
98 induce any fitness cost (23, 24). *Per os* provisioned rec*Sodalis* remains only in the gut (23).
99 'Paratransgenic' tsetse flies that house rec*Sodalis* have been successfully used to deliver anti-
100 trypanosomal nanobodies (25-27). Paratransgenesis has also been used to deliver dsRNA for

101 gene silencing in kissing bugs (28, 29) and in the malaria mosquito *Anopheles gambiae* (30, 31).
102 However, paratransgenic expression of small RNA antagonists to knockdown miRNA expression
103 has not been reported to date. Herein we engineered *Sodalis* to paratransgenically express
104 three tandem antagonist-275 repeats (3xant-*miR275*) in tsetse's cardia and midgut
105 environments, and then used this experimental system to investigate the mechanism(s) by
106 which *miR275* regulates the physiological homeostasis of the fly's gut environment. We found
107 that paratransgenic flies presented multiple phenotypes that are associated with the
108 production of a structurally compromised PM barrier and/or disrupted gut homeostasis. Our
109 novel paratransgenic expression system can be applied to further study functions of microRNAs
110 that are involved in the tsetse-trypanosome interaction, thus advancing our understanding of
111 parasite-deployed strategies to manipulate its host physiology. Additionally, this method could
112 be broadly applied to other arthropod systems where a host interacts with microbes (especially
113 with non-model systems where host genetic manipulation can be difficult), which could be
114 particularly useful to study pathogen-host interactions in the field of vector biology.

115 **2. Materials and methods**

116 *2.1 Tsetse fly and bacterial cultures*

117 Tsetse flies (*Glossina morsitans morsitans*) were reared in the Yale University insectary at 25°C
118 and 70% relative humidity (RH), and received defibrinated bovine blood every 48 h via an
119 artificial blood feeding system. Wild-type *Sodalis glossinidius morsitans* were isolated from
120 surface-sterilized *Gmm* pupae and plated on Difco™ Brain Heart Infusion Agar (BD Biosciences)
121 plates that were supplemented with 10% bovine blood (BBHI). Clonal *Sodalis* populations were
122 subsequently maintained *in vitro* in Bacto™ Brain Heart Infusion (BHI) medium (BD biosciences)
123 at 26°C, 10% CO₂.

124

125 *2.2. Generation of recSodalis strains*

126 To generate rec*Sodalis*, two constructs (Fig. 1A) were made using a modified pgRNA-bacteria
127 plasmid (NEB, Addgene plasmid # 44251). This plasmid, which encodes an ampicillin resistance
128 cassette, was originally designed to express short guide RNAs for CRISPR application and is thus
129 well suited for expressing small RNAs (32). An additional endonuclease cut site Sbfi was built
130 into the original pgRNA plasmid backbone so as to include an RNA terminator sequence in the
131 modified plasmid. Two pairs of two complementary single-stranded oligonucleotides (oligos)
132 that encode either three copies of the *miR275* antagonir (3xant-*miR275*) or the scrambled
133 *miR275* control (Scr-275) were synthesized at Yale Keck Oligo Synthesis Resource (Table 1). The
134 two complementary single-stranded oligos, each of which encode Spel and Sbfi restriction
135 endonuclease cut sites, were annealed at 95°C for 5 min, cooled to room temperature for 30
136 min and stored at -20°C for future use. Both pgRNA and the double stranded miRNA-encoding

137 oligos were subjected to restriction endonuclease treatment by SpeI and SbfI at 37°C for 2 h.

138 The oligos were then ligated into pgRNA using T4 DNA ligase (NEB), and the constructs were

139 propagated in *E. coli* DH5α cells. All purified plasmid constructs were sequenced at Yale's Keck

140 Sequencing Laboratory to confirm their structure.

141 **Table 1. Oligonucleotide sequences.** Capitalized letters represent restriction endonuclease cut

142 sites. Red = antagomir-275.

Name	Strand	Sequence
3xant- <i>miR275</i>	F	CTAGT cgcg ctacttcaggtacctgaat cgcg ctacttcaggtacctgaatccgcgcgcacttcag
	R	gtacctga CCTGCAGGtcaactgaaaaagtggcaccgagtcggtgcttttga AGCTtcaaaaaagcaccgactcgggccactttcaagttgaCCTGCAGG tcaggtacctgaagtagcgcg
Scr-275	F	CTAGTaccggcttagtaagaggctagtttagcatcacgtttccatggctcaatggcataggatgtcggttgg cggtcgggacctcgcaagagattaaCCTGCA
	R	GGtaatctctgcgaggccacacgccaacgaacgacatcctatgcattgagcaaaatggaagacgtgtat ctaactagccttactaagccggtA

143

144 The purified DNA plasmids were electroporated into wild-type *S. glossinidius morsitans*

145 (*Sgm*^{WT}) as described previously (33). Two *recSodalis* strains were used in this study: 1) *Sgm*^{3xant-}

146 *miR275*, which encodes 3xant-*miR275*, and 2) the *miR275* scrambled control (*Sgm*^{Scr-275}) (Table 1).

147 In brief, 25 mL of log-phase *Sodalis* cells (OD₆₀₀ = 0.3~0.5; SmartSpec Plus spectrophotometer;

148 Bio-Rad, Hercules, CA) were washed consecutively in 25 mL, 1 mL and 1 mL 10% sterile pre-

149 chilled glycerol. After the three washes, the *Sodalis* cell pellets were resuspended in 50 μL

150 sterile 10% glycerol. Each 50 μ L of cell mixture was mixed with 1 or 2 μ L (\sim 100 ng) of plasmid
151 DNA and subjected to electroporation (voltage, 1.9 kV; capacitance, 25 μ F; resistance, 200
152 omega). After electroporation, the *recSodalis* cells were immediately placed in 5 mL BHI
153 medium for overnight recovery at 26°C, 10% CO₂. The recovered cells were then plated on BHI
154 plates supplemented with 10% bovine blood, and transformants were selected with ampicillin
155 (50 μ g/mL). After a 1-week incubation, transformants were selected for PCR and sequencing.
156 After the sequence was confirmed, a single *recSodalis* colony was grown in BHI medium for
157 future experiments.

158

159 *2.3 Establishment of paratransgenic tsetse flies*
160 To generate paratransgenic tsetse flies, two groups of teneral female flies (newly emerged
161 unfed adults) were given two consecutive blood meals (separated by 1 day) containing either
162 *Sgm*^{3xant-miR275} or *Sgm*^{Scr-275} (10⁶ CFU/mL each in the first two blood meals) and ampicillin (50
163 μ g/mL). After a third blood meal (no *recSodalis*, no ampicillin), 8-day old paratransgenic flies
164 were used in the experiments described below. All plasmid constructs, as well as *recSodalis*
165 strains and paratransgenic tsetse lines, are summarized in Table 1.

166

167 *2.4 Gentamicin exclusion assay and quantification of recSodalis*
168 Gentamicin is unable to cross the eukaryotic cell wall and hence only kills extracellular bacteria
169 (34). Cardia and midgut tissues were dissected from 8-day old paratransgenic and incubated in
170 sterile 0.85% NaCl supplemented with 100 μ g/mL gentamicin. Controls were incubated in the
171 sterile NaCl in the absence of gentamicin. Tissues were agitated on a shaking platform at room

172 temperature for 1 h and washed 4 times in 500 μ l sterile 0.85% NaCl. After the 4th wash, tissues
173 were rigorously homogenized in sterile 0.85% NaCl. 50 μ l of lysate from each treatment was
174 plated onto BHI Agar plates supplemented with 10% blood and 50 μ g/mL ampicillin. After 7
175 days of incubation at 26°C, 10% CO₂, colonies on each plate were counted as described in (23).
176 Multiple colonies were randomly selected for colony PCR (with primers targeting the inserted
177 section of the pgRNA plasmid) and subjected to sequencing to confirm they housed the correct
178 plasmid construct.

179

180 *2.5 Dual luciferase reporter assay*

181 To clone the 3xant-*miR*-275 into psiCheck-2 (Promega), two complementary single-stranded
182 oligos that encode 3xant-*miR*-275 and Xhol and NotI restriction endonuclease cut sites were
183 synthesized at Yale Keck Oligo Synthesis Resource (Table 1). The complementary oligos were
184 annealed at 95°C for 4 min and cooled to room temperature for 30 min. The psiCheck-2 vector
185 and the doubled stranded miRNA-encoding oligos were subjected to Xhol and NotI treatment at
186 37°C for 2 h followed by inactivation at 65°C. The oligos were then ligated into the double
187 digested psiCheck-2 plasmid using T4 DNA ligase (NEB) at room temperature for 2 h, and the
188 constructs were propagated in *E. coli* DH5 α cells. All purified plasmid constructs were
189 sequenced at Yale's Keck Sequencing Laboratory to confirm their structure. The psiCheck-2
190 vector containing the 3xant-*miR*275 sequence is hereafter referred to as psiCheck-2^{3xant-*miR*275}.

191 For transfection, *Drosophila* S2 cells (Invitrogen) were maintained at 28°C in Schneider
192 *Drosophila* medium supplemented with 10% heat inactivated FBS. We co-transfected 100 ng of
193 psiCheck-2^{3xant-*miR*275} and the synthetic tsetse *miR*275miScript miRNA mimic at 100 nM (Qiagen)

194 or with AllStars Negative Control (Qiagen) into S2 cell lines using Attractene Transfection
195 reagent following the manufacturer's protocol (Qiagen). A "no miRNA" treatment with only
196 psiCheck-2 plasmid and transfection reagent was also conducted. Dual luciferase reporter
197 assays were performed 48 h post transfection using the Dual Luciferase Reporter Assay System
198 following the manufacturer's protocol (Promega). The *renilla* (primary reporter) luciferase
199 signal was normalized to the *firefly* (internal control) luciferase signal. Each treatment was
200 conducted triplicate.

201

202 *2.6 Quantitative real-time PCR*

203 Quantitative real-time PCR (qPCR) was used to quantify the expression levels of miR275, non-
204 coding small nuclear RNA (snRNA) *U6*, and saliva-associated genes in our paratransgenic flies
205 (described in section 2.3 above). Tsetse cardia, midgut and salivary glands were microscopically
206 dissected 24-48 h after the third blood meal. Total RNA was extracted from pools of 5 cardia, 5
207 midgut or 10 salivary glands (as one biological replicate) using Trizol reagent (35). RNA was
208 cleaned and purified using an RNA Clean and Concentrator Kit with in-column DNase treatment
209 (Zymo Research). RNA quality and quantity was quantified using a NanoDrop 2000c (Thermo
210 Scientific). A small portion of the RNA was then reverse transcribed into cDNA using the
211 miScript II RT kit (Qiagen 218160) followed by qPCR. For each sample, two technical replicates
212 were used. Relative expression (RE) was measured as $RE = 2^{-ddCT}$, and normalization was
213 performed using *U6* gene expression as a reference. Primers for amplifying *miR275*, saliva-
214 associated genes and the reference gene are listed in Table S1.

215 qPCR was performed on a CFX96 PCR detection system (Bio-Rad, Hercules, CA) under
216 the following conditions: 8 min at 95 °C; 40 cycles of 15 s at 95 °C, 30 s at 57 °C or 55 °C, 30 s at
217 72 °C; 1 min at 95 °C; 1 min at 55 °C and 30 s from 55 °C to 95 °C. Each reaction consisted of 10
218 µl: 5 µl of iTaq™ Universal SYBR® Green Supermix (Bio-Rad), 1 µl cDNA, 2 µl primer pair mix (10
219 µM) and 2 µl nuclease-free H₂O.

220

221 *2.7 Tsetse whole gut weight measurements*

222 Individual guts from 8-day old paratransgenic flies (*n*=20 per group) were dissected 24 h after
223 their last blood meal and weighed with a digital scale as an indicator for blood digestion.

224

225 *2.8 Serratia infection assay*

226 8-day old paratransgenic individuals were fed a blood meal containing 10³ CFU/mL *S.*
227 *marcescens* strain Db11. Thereafter, all flies were maintained on normal blood and their
228 mortality was recorded every other day for 14 days. Details of the *Serratia* infection assay are
229 provided in (7, 10, 11).

230

231 *2.9 Trypanosome infection prevalence*

232 The 8-day old paratransgenic flies were challenged *per os* with a blood meal containing 10⁷
233 CFU/mL *Trypanosoma brucei brucei* strain 503 supplemented with 0.9 mg/mL of cysteine.
234 Thereafter, the flies were maintained on normal blood meals for two weeks. Their guts were
235 dissected and microscopically examined to determine trypanosome infection status.

236

237 *2.10 mRNA library construction and RNA sequencing*

238 Two groups of paratransgenic flies (*Gmm*^{3xant-miR275} vs. *Gmm*^{Scr-275}) were generated as described
239 in Section 2.3. All flies were dissected 36 h after the third blood meal; 10 individual cardia or 5
240 individual midgut were pooled as one biological replicate and stored in -80°C prior to RNA
241 extraction, a total 3 biological replicates per treatment were used. Total RNA was extracted
242 using Trizol reagent according to the manufacturer's protocol (Invitrogen), followed by RNA
243 Clean and Concentrator Kit and in-column DNase treatment (Zymo Research). RNA quality and
244 quantity were quantified using a bioanalyzer. All 6 mRNA libraries were prepared and
245 sequenced (pair-ended) at Yale Center for Genome Analysis (YCGA) using Illumina NovaSeq
246 system.

247

248 *2.11 RNA-seq data processing*

249 RNA-seq raw reads were uploaded to FastQC (v. 0.11.9,
250 www.bioinformatics.babraham.ac.uk/projects/) for quality check, and then trimmed and
251 filtered to remove ambiguous nucleotides and low-quality sequences. The reads were mapped
252 to *Glossina morsitans morsitans* reference genome (36) using HISAT2 v2.1.0 with default
253 parameters (37, 38). We then used the function 'htseq-count' in HTSeq v0.11.2 (39) to count
254 the number of reads mapped to the genes annotated in the reference genome (version
255 GmorY1.9 at Vectorbase.org) with option "-s reverse". Reads that were uniquely aligned to
256 *Gmm* transcripts were used to calculate differential gene expression using *EdgeR* package in R
257 software (40). Significance was determined using EdgeR General linear models, corrected with a
258 False Discovery Rate (FDR) at p < 0.05. The differentially expressed (DE) genes were uploaded to

259 VectorBase (<http://beta.vectorbase.org>) for gene ontology (GO) enrichment analysis using the
260 built-in web tool GO Enrichment analysis. REVIGO was used to remove the redundant GO terms
261 (41).

262

263 *2.12 Replicates and statistics*

264 Biological replicates were obtained from samples derived from distinctly repeated experiments.
265 Details about sample sizes and statistical tests used for data analyses in this study are indicated
266 in the corresponding figure legends.

267 **3. Results**

268 **3.1. Successfully developed the paratransgenic expression system**

269 To knock down expression of tsetse *miR275*, we designed two expression constructs that
270 encode 1) 3xant-*miR275* to knockdown *miR275*, and 2) a scrambled miRNA sequence (Scr-275)
271 that served as the control. Individual clonal populations of wild-type *Sodalis* (*Sgm*^{WT}) were
272 transformed with one of the plasmids and are henceforth designated *Sgm*^{3xant-*miR275*} and *Sgm*<sup>Scr-
273 275</sup> (Fig. 1A). We then colonized individual groups of newly eclosed (teneral) adult tsetse *per os*
274 with either *Sgm*^{3xant-*miR275*} or *Sgm*^{Scr-275}, thus generating paratransgenic tsetse cohorts
275 designated *Gmm*^{3xant-*miR275*} (treatment) and *Gmm*^{Scr-275} (control), respectively. During the
276 development of the paratransgenic lines, we supplemented the first two bloodmeals with
277 ampicillin to suppress the *Sgm*^{WT} population, which provided the antibiotic-resistant *recSodalis*
278 populations a selective advantage over the indigenous antibiotic susceptible WT cells.

279 We performed gentamicin exclusion assays to confirm that the *recSodalis* successfully
280 invaded tsetse cardia and midgut cells. Gentamicin cannot penetrate eukaryotic cell
281 membranes, and thus treatment with this antibiotic effectively eliminates the extracellular
282 bacteria but leaves the intracellular population intact (34). We incubated separate cardia and
283 midgut tissues dissected from 8-day old paratransgenic flies in either gentamicin (treatment) or
284 PBS (control). Tissues were subsequently rinsed, homogenized, and plated on BBHI plates
285 supplemented with ampicillin. We recovered 214 (\pm 54.0) and 9.7×10^5 (\pm 9.6×10^4) gentamicin-
286 resistant CFU from the cardia and midgut tissues, respectively (Fig. 1B). Sequencing of the
287 transformation plasmid from several bacterial clones confirmed their identity as either *Sgm*<sup>3xant-
288 *miR275*</sup> or *Sgm*^{Scr-275}. These findings indicate that *recSodalis* was successfully internalized by tsetse

289 cardia and midgut cells where they were protected from the antibacterial effects of gentamicin.
290 Additionally, significantly more rec*Sodalis* cells were present within midgut cells than cells of
291 the cardia organ. We similarly quantified the *Sgm*^{3xant-miR275} and *Sgm*^{Scr-275} present in the no
292 gentamicin control groups (cardia, 684 ± 90 , $p = 0.002$; midgut, $2.0 \times 10^6 \pm 1.1 \times 10^5$, $p < 0.0001$)
293 (Fig. 1B), and found that 31% and 49% of rec*Sodalis* present in the gut were intracellular within
294 cardia and midgut tissues, respectively. These data also indicated that our rec*Sodalis*
295 successfully reside within tsetse's gut at a density similar to that of indigenous *Sgm*^{WT} in age-
296 matched flies (23). Thus, we demonstrated that rec*Sodalis* successfully colonized tsetse's gut
297 where they reside within cells that comprise the fly's cardia and midgut tissues.

298 To test the binding efficacy of the antagonists expressed by 3xant-*miR275* to tsetse's
299 mature *miR275*, we performed a dual luciferase reporter assay. We cloned the 3xant-*miR275*
300 construct into the multiple cloning site located in the 3'-UTR region of the reporter gene
301 (*renilla*) in the psiCheck-2 vector (psiCheck-2^{3xant-miR275}). When *miR275* binds to the sponge
302 construct cloned in the 3'UTR region of the reporter gene (which initiates the RNA interference
303 (RNAi) process), we expect the *renilla* transcript to be degraded, and the *renilla* Luciferase
304 signal to be decreased. The psiCheck-2 vector also contains a *firefly* reporter in the expression
305 cassette that is designed to be an intra-plasmid transfection normalization reporter. Thus, the
306 *Renilla* luciferase signal is normalized to the *firefly* signal to standardize between different
307 biological samples. We measured luciferase activity in three different experiments: 1) psiCheck-
308 2^{3xant-miR275} + synthetic *miR275* mimic, 2) psiCheck-2^{3xant-miR275} + synthetic AllStars Negative
309 Control, and 3) psiCheck-2^{3xant-miR275} alone, and we found that the relative luciferase activity
310 (*renilla*/*firefly*) was significantly suppressed in experiment 1 compared to experiments 2 and 3

311 (p< 0.05 and p<0.0005, respectively; Fig. 1C). In other words, in the presence of synthetic
312 *miR275* mimic, the luciferase activity was significantly repressed, which indicated that our
313 sponge construct was successful when tested *in vitro* using an insect cell line. This outcome
314 demonstrated that the *miR275* effectively binds to the *miR275* sponge and initiates the RNAi
315 process with its associated mRNA.

316 To confirm the knockdown effect of *miR275* levels *in vivo*, we used qPCR to quantify the
317 relative expression of *miR275* in *Gmm*^{3xant-*miR275*} (treatment) and *Gmm*^{Scr-275} (control)
318 individuals. Using multiple biological samples (each of which contained 5 dissected tissues
319 pooled per sample) to reduce variability, we confirmed that the expression level of *miR275* was
320 significantly reduced in the midgut of the treatment group compared to that of the control
321 group (p < 0.05; Fig. 1D). However, our qPCR results did not consistently reveal a significant
322 reduction of *miR275* levels in the cardia organ of treatment versus control paratransgenic
323 tsetse (Fig. 1E).

324

325 **3.2 *Gmm*^{3xant-*miR275*} gut physiological homeostasis is compromised**

326 We demonstrated that *recSodalis* successfully invaded tsetse cardia and midgut tissues, and
327 that *miR275* was knocked down in the midgut of *Gmm*^{3xant-*miR275*}. We next sought to determine
328 if midgut physiologies, such as blood meal digestion and PM functional integrity, were impaired
329 in *Gmm*^{3xant-*miR275*} flies in a manner similar to what was observed when tsetse *miR275* (11) and
330 mosquito *Ae. aegypti* *miR275* (17) were depleted through the use of synthetic *miR275*
331 antagonirs. We compared the weight of midguts from 14 individual 8-day old *Gmm*^{3xant-*miR275*}
332 and *Gmm*^{Scr-275} flies 24 h after their last blood meal. We observed that guts from *Gmm*^{3xant-*miR275*}

333 individuals weighed significantly more (8.37 ± 0.64 mg) than did those from *Gmm*^{Scr-275} controls
334 (4.03 ± 0.56 mg) ($p < 0.001$; Fig. 2A), thus indicating that blood digestion and/or excretory
335 processes (diuresis) were greatly disrupted in *Gmm*^{3xant-miR275}.

336 We next employed a highly sensitive *Serratia* infection assay to test whether PM
337 structural integrity was compromised in paratransgenic *Gmm*^{3xant-miR275} compared to *Gmm*^{Scr-275}
338 flies. We observed that 22% of *Gmm*^{3xant-miR275} individuals survived for 19 days following *per os*
339 challenge with *Serratia*. Comparatively, 0% of *Gmm*^{Scr-275} control flies survived this challenge (p
340 < 0.0001 ; Fig. 2B). These data indicate that paratransgenic-mediated repression of *miR275*
341 expression impairs tsetse's gut physiology and results in the production of a functionally
342 compromised PM barrier, similar to what we had observed using synthetic antagonists provided
343 *per os* in a single bloodmeal (11).

344 Trypanosome infection establishment success in tsetse's midgut inversely correlates
345 with the structural integrity of the fly's PM (7, 42). We next evaluated trypanosome infection
346 outcomes in the midgut of *Gmm*^{3xant-miR275} relative to *Gmm*^{Scr-275} control individuals to further
347 confirm that paratransgenic expression of *miR275* sponges interferes with the efficacy of
348 tsetse's PM structure. We provided 8-day old adult paratransgenic flies a blood meal containing
349 cysteine, which inhibits trypanolytic antioxidants present in the tsetse's midgut (10, 43), and
350 10^7 *T. b. brucei*/mL of blood. Thereafter, the flies were maintained on normal blood meals for
351 two weeks and subsequently dissected and microscopically examined to determine their
352 midgut infection status. We found that significantly more *Gmm*^{3xant-miR275} individuals (49%)
353 hosted trypanosome infections in their gut than did their *Gmm*^{Scr-275} counterparts (11%) ($p <$
354 0.0001 ; Fig. 2C). The higher parasite infection prevalence we observed in *Gmm*^{3xant-miR275}

355 individuals further signifies that the functional integrity of tsetse's PM is significantly
356 compromised when *miR275* sponges are paratransgenically expressed in the fly's midgut.

357

358 **3.3 Global gene expression profiling in paratransgenic cardia and midgut**

359 Our paratransgenic expression system has confirmed prior phenotypes that we observed
360 following *per os* administration of synthetic antagonir-275, including a significant reduction of
361 *miR275* expression in the midgut and modified phenotypes associated with compromised gut
362 physiological homeostasis such as dysfunctional digestive processes and compromised PM
363 functional integrity. Additionally, we observed higher trypanosome infection prevalence in the
364 midgut of *Gmm*^{3xant-miR275} compared to *Gmm*^{Scr-275} flies. To obtain a broader understanding of
365 the molecular mechanisms and pathways that are regulated by *miR275*, we performed global
366 transcriptomic profiling in cardia and midgut tissues that were harvested from paratransgenic
367 *Gmm*^{3xant-miR275} relative to *Gmm*^{Scr-275} controls. All flies were age matched and inoculated *per os*
368 with their respective *recSodalis* strains in their 1st and 2nd blood meals. For both comparisons
369 each biological replicate (*n*=3) contained pooled midguts (*n*=5) or cardia (*n*=10) tissues from 8-
370 day old adults 36 h after their third blood meal. A total of 12 mRNA libraries were sequenced,
371 and the total reads and uniquely mapped reads from each are summarized in Table S2. We
372 generated multi-dimensional scaling (MDS) plots to understand the overall gene expression
373 differences between the biological replicates and treatment groups. We found that all three
374 replicates within each treatment group clustered closely together as did all control group
375 replicates (Fig. 3A-B). When comparing gene expression differences in the cardia, we found that
376 265 genes (out of a total of 6101) were differentially expressed (DE; FDR< 0.05), with 99 (1.6%)

377 and 166 (2.7%) up- and down-regulated in *Gmm*^{3xant-*miR275*} relative to that of *Gmm*^{Scr-275} control
378 individuals, respectively (Fig. 3A). When comparing gene expression differences in midgut
379 samples, we found that 283 genes (out of a total of 5540) were DE (FDR < 0.05), with 116 (2.1%)
380 and 167 (3.0%) up- and down-regulated in the midgut of *Gmm*^{3xant-*miR275*} relative to *Gmm*^{Scr-275}
381 individuals, respectively (Fig. 3B).

382

383 **3.4 Gene Ontology (GO) enrichment analysis in the paratransgenic cardia and midgut**
384 We next applied GO enrichment analyses to acquire broad insights into the functional
385 contributions of the DE genes we identified. In the 99 up-regulated transcripts of *Gmm*^{3xant-*miR275*}
386 cardia relative to controls, enriched GO terms included chitin binding in the molecular function
387 category, whereas in the 166 down-regulated transcripts, enriched GO terms included iron
388 binding, heme binding, adenosine deaminase activity, and hydrolase and peptidase activity (Fig.
389 4A; Table S3). In the 116 upregulated transcripts of *Gmm*^{3xant-*miR275*} midguts relative to controls,
390 enriched GO terms included catalytic activity, oxidase activity and peptidase activity in the
391 molecular function category, while in the downregulated transcripts, enriched GO terms
392 included ribosome and cellular component biogenesis in biological processes (Fig. 4B; Table S3).

393

394 **3.5 Analysis of DE genes in the cardia from *Gmm*^{3xant-*miR275*} vs. *Gmm*^{Scr-275} control**
395 Given that our phenotypic analysis indicated that *miR275* is involved in blood digestion and PM
396 barrier function (Fig. 2), we first evaluated the DE genes whose products are likely associated
397 with these functions. Among the genes whose putative products have been identified as PM
398 structural proteins through proteomics analysis of the PM (44), we found that tsetse EP, midgut

399 trypsin (GMOY007063) and choline acyltransferase were significantly down-regulated, while
400 serine type endopeptidase (GMOY009757), *pro1* and *GmmPer12* were up-regulated in
401 *Gmm*^{3xant-miR275} relative to *Gmm*^{Scr-275} controls (Fig. 5A; Table S4). Among the secreted products
402 localized to the PM, we found several digestive enzymes, serine proteases (Sp), trypsin and
403 peptidases for which transcript abundance was significantly reduced in the treatment group
404 (Fig. 5A; Table S4). The reduction in the production of these gene products may account for the
405 impaired blood digestion we noted in *Gmm*^{3xant-miR275} individuals. The down-regulation of
406 several genes whose products are associated with the PM, such as tsetse EP, midgut trypsin, *Sp*
407 (GMOY006839), *Sp15*, and choline acyltransferase, were also noted from trypanosome-infected
408 flies where PM functions were also compromised (10). Tsetse EP protein is localized to the
409 midgut, PM, and hemolymph (45, 46). The gene that encodes this protein is immune
410 responsive, as its expression level was upregulated in response to bacterial challenge (45).
411 Furthermore, when tsetse EP was depleted via RNAi, trypanosome infection prevalence
412 significantly increased (46).

413 Interestingly, the expression of chitinase (GMOY005519) and chitin binding protein
414 (GMOY011054) was significantly upregulated in the cardia of *Gmm*^{3xant-miR275} individuals.
415 Different from other arthropod vectors, such as mosquitoes and sandflies, adult tsetse flies
416 have type II PM, which is continuously secreted by cells located within the cardia. The PM is
417 composed of a lattice of chitin fibrils cross linked by glycoproteins (Peritrophins) that contain
418 chitin binding domains (CBD) (47). Chitin is an extracellular polysaccharide that can be
419 enzymatically hydrolyzed by chitinases (48). Prior studies on trypanosome-infected cardia (10)
420 and midguts (49) also indicated upregulated expression of chitinases, which likely resulted in

421 compromised PM integrity. The reduction in PM associated gene expression, and the
422 upregulation of the putative chitin degrading products, may contribute to the loss of PM
423 integrity observed in paratransgenic *Gmm*^{3xant-miR275}.

424 With respect to blood digestion processes, we detected 10 transcripts involved in heme
425 binding and detoxification processes that were downregulated in *Gmm*^{3xant-miR275} compared to
426 controls (Fig. 5B; Table S4). Among these putative products were cytochrome (CYP) P450
427 enzymes, which belong to a superfamily involved in insect metabolism, detoxification and
428 insecticide resistance in many different species (50), as well as several CYPs regulated by
429 *Plasmodium* (51) and trypanosome (52) infections. Heme in the blood can induce oxidative
430 damage to insect tissues (53) and the presence of heme binding proteins in *Ae. aegypti* PM
431 suggest the structure exhibits a detoxification role (54).

432 Among the transcripts encoding transporters and/or transmembrane channel proteins
433 that would be involved in secreting, trafficking and absorbing digestive products, we detected
434 12 that were downregulated and 10 that were upregulated in *Gmm*^{3xant-miR275} relative to
435 controls (Fig. 5C; Table S3). These up and down-regulated genes encode functions that involve
436 transporting nutrients such as sugar and amino acids (e.g., major facilitator super family sugar
437 transporter, glucose transporter, *Slif* and *minidiscs*), ions and water (e.g., Na/phosphate
438 cotransporter, calcium channel, *Kir* family member, magnesium transporter, and aquaporin),
439 and organic compounds (e.g. folate transporter). Annexin and Innexin are both upregulated in
440 *Gmm*^{3xant-miR275}. Annexin belongs to a large calcium dependent membrane binding protein
441 family and the functions range from receptors of proteases in the gut epithelium to inhibitors of
442 blood coagulation (55). *Plasmodium* ookinetes use annexin for protection or to facilitate their

443 development in the mosquito gut (56). Annexin is upregulated in trypanosome-infected salivary
444 glands (SG) (52). Innexin proteins form gap junction channels and play critical roles in cell-to-
445 cell communication in a variety of physiology activities (57). Innexin 2 is a target gene of the
446 *Wingless* signaling pathway in the proventricular cells in *Drosophila* (58). One innexin was DE
447 upon trypanosome infection in tsetse, *Glossina fuscipes fuscipes* (59).

448 We also noted 19 abundant and significantly downregulated transcripts encoding
449 secreted proteins in *Gmm*^{3xant-miR275} cardia (Fig. 5D; Table S4), including Adenosine deaminase-
450 related growth factor 3 (*Adgf3*; FC= 4.94x10⁻⁶ and FDR= 1.00x10⁻¹⁵²), salivary gland protein 3
451 (*SGP3*; FC= 6.24x10⁻⁵ and FDR= 1.64x10⁻¹²²), antigen-5 precursor (*Ag5*; FC= 1.21x10⁻³ and FDR=
452 2.86x10⁻¹⁰³), *Tsal1* protein precursor (FC= 2.21x10⁻⁴ and FDR= 1.26x10⁻⁶¹), 5'-nucleotidase
453 (5'Nuc; FC= 1.18x10⁻⁴ and FDR= 1.10x10⁻⁴⁷), *Adgf2* (FC= 2.25x10⁻⁵ and FDR= 2.49x10⁻³⁶) and one
454 of the two *Tsal2* protein precursors (GMOY012361) (FC= 5.81x10⁻⁵ and FDR= 1.86x10⁻³⁴) (Table
455 S4). All of these 19 genes are preferentially expressed in SG tissue and downregulated in
456 trypanosome-infected SGs (52, 60, 61). Interestingly, our previous study with parasite-infected
457 cardia also indicated that 9 of these genes [*Adgf3*, *Ag5*, *Tsal1*, *Tsal2* (GMOY012360), *SGP1*,
458 tsetse thrombin inhibitor (*TTI*), salivary secreted protein (GMOY012067) and two secreted
459 proteins (GMOY003214 and GMOY007077)] are expressed in the cardia, and 4 of them [*Ag5*,
460 *Tsal2*, *TTI* and one of the secreted proteins (GMOY007077)] are significantly impacted by
461 trypanosome infection (10). Moreover, our earlier transcriptomic analysis of trypanosome-
462 challenged tsetse guts (48 h post provisioning of a parasite containing bloodmeal) has revealed
463 that the expression of sixteen of these genes [*Tsal1*, *TTI*, *SGP1*, *GRP2*, 5' Nuc, both *Tsal2*s,
464 *Adgf1*, *Adgf2*, *Adgf3*, *Adgf5*, salivary secreted protein and two secreted peptides (GMOY003214

465 and GMOY012286)] are significantly reduced relative to unchallenged controls (11). All of these
466 SG preferential gene products were previously detected in tsetse saliva and thought to be
467 essential for the fly's ability to successfully blood feed (62). Adgf, TTI and 5'Nuc are associated
468 with anticoagulant functions in tsetse's saliva and gut (59, 60, 63-65), while Ag5 is a major
469 allergen involved in hypersensitivity reactions in the mammalian host (66).

470 Lastly, six DE genes in *Gmm*^{3xant-*miR275*} flies encoded products associated with
471 embryogenesis and imaginal cell proliferation. Among these genes, forkhead and wing blister
472 (*Wb*) were downregulated, while imaginal disc growth factor (*Idgf*), GMOY004790 (homologous
473 to integrin in *Md*), wingless (*Wg*), and *Wnt6* were upregulated (Table S4). *Idgf* is involved in
474 extracellular matrix formation in insects and participates in critical physiological activities such
475 as larval and adult molting and wing development (67). The wingless pathway is an intracellular
476 signaling network; *Wg* signaling in *Drosophila* involves embryonic epidermis and wing imaginal
477 disc (68). Interestingly, *Wg* expression was reduced when tsetse *miR275* was knocked down
478 using the synthetic antagonir treatment (11), contrary to our data presented here using the
479 constitutive silencing approach, which shows higher levels of *Wg*.

480

481 **3.6 Analysis of DE genes in the midgut from *Gmm*^{3xant-*miR275*} vs. control *Gmm*^{Scr-275}**

482 Similar to our analysis with the cardia, we first analyzed DE genes that are associated with PM
483 components and digestive enzymes in *Gmm*^{3xant-*miR275*} midgut transcriptomes. Among previously
484 identified PM products (44), we found 7 that were upregulated in *Gmm*^{3xant-*miR275*} midguts,
485 including *pro2*, *pro3*, *Sp6*, choline acetyltransferase, chitin deacetylase, midgut trypsin
486 (GMOY007063), and a serine type endopeptidase (GMOY9757) (Table S5). In addition, we also

487 identified several digestive enzymes, including trypsin, proteases and peptidases that were
488 upregulated in *Gmm*^{3xant-miR275} midguts relative to the controls (Fig. 6A; Table S5). *Pro3*, *Sp6* and
489 serine type endopeptidase (GMOY009757) were upregulated in response to *T. brucei*
490 *gambiense* (*Tbg*) infection (49). Higher levels of Chitin deacetylase, a hydrolytic enzyme that
491 catalyzes the acetamido group in the N-acetylglucosamine units of chitin (69), could contribute
492 to a compromised PM, similar to what we report for *chitinase* expression in the paratransgenic
493 cardias above. The increased midgut weight we observed in *Gmm*^{3xant-miR275} flies could reflect a
494 dysfunctional gut enzyme production and/or altered enzyme transport in response to the
495 compromised PM integrity.

496 Among the twenty genes encoding transporters and/or transmembrane channel
497 proteins DE in the midgut (Fig. 6B; Table S5), two (GMOY012503 and GMOY010388) were also
498 identified DE in the cardia of *Gmm*^{3xant-miR275}. In addition to transporters, we noted 7 DE genes,
499 including down regulated members of *CYP* p450, ubiquitin ligase and up regulated nitric-
500 oxidase synthase (*NOS*) that are associated with heme binding and oxidative response (Fig. 6C;
501 Table S5). The ubiquitin ligase and a heme binding protein (GMOY001150) were also down
502 regulated in the cardia of *Gmm*^{3xant-miR275}. Ubiquitin ligase and *CYP* p450, which are associated
503 with insecticide resistance and metabolism of natural or xenobiotic products in many insect
504 species (70), have been linked to toxin metabolism following a blood meal in *An. gambiae* (71).
505 *CYP* p450-4g1 is also DE (FC>2) in response to *Tbg* infections in the *Gmm* midgut (49). *NOS* is
506 responsible for producing cellular nitric oxide, which is trypanocidal (72). *NOS* expression is
507 down regulated in trypanosome-infected SGs (52) and cardia (10, 73), and VSG-treated cardia
508 as well (11)

509 Among the SG preferential genes that are dramatically reduced in *Gmm*^{3xant-*miR275*} cardia,
510 we detected five that were expressed in the midgut: *salivary C-type lectin* (GMOY000466), *Ag5*,
511 secreted peptides (GMOY007065 and GMOY007077) and *TTI*. However, only the salivary C-type
512 lectin was DE in the midgut and upregulated in *Gmm*^{3xant-*miR275*} relative to controls.

513

514 **3.7 The paratransgenic knockdown effect is gut tissue specific**

515 We observed the significant downregulation of 19 SG preferential genes in the cardia
516 transcriptome from *Gmm*^{3xant-*miR275*} versus *Gmm*^{Scr-275} flies. Because *per os* provisioned
517 *recSodalis* is restricted in the gut tissue not in the hemolymph (23), we tested whether *miR275*
518 is expressed in the SG (Fig. 7A). We anticipated that the *miR275* knockdown effects would be
519 restricted to the gut and not impact gene expression levels in other organs. To confirm this, we
520 investigated whether paratransgenic knockdown of *miR275* in tsetse's cardia induces a systemic
521 response that results in the knockdown of these genes in the fly's SGs. We first dissected the SG
522 organ from *Gmm*^{3xant-*miR275*} paratransgenic flies and tested the *miR275* expression levels. We
523 subsequently monitored the expression of *Adgf3* (GMOY012374), *Adgf5* (GMOY012375) and
524 *SGP1* (GMOY012268), which are abundantly expressed in tsetse's SGs (52, 60, 61) and
525 downregulated in *Gmm*^{3xant-*miR275*} cardia. We found that none of the three SG-preferential genes
526 were significantly reduced in the SG of *Gmm*^{3xant-*miR275*} individuals despite being significantly
527 down-regulated in the cardia (Fig. 7B-D). These results indicate that the effect of the
528 paratransgenic knockdown is restricted to tsetse's gut tissues where *recSodalis* reside, and does
529 not impact gene expression at the systemic level.

530

531 **4. Discussion**

532 We developed a paratransgenic expression system using tsetse's endosymbiont *Sodalis* to
533 experimentally modify *miR275* transcript abundance in tsetse's gut and to investigate the
534 resulting physiological impact. Specifically, we engineered *Sodalis* to express *miR275* sponges (3
535 tandem antagomir-275 repeats), and demonstrated that the rec*Sodalis* successfully colonize
536 tsetse's cardia and midgut where they invade resident epithelial cells. We then demonstrated
537 that the *miR275* sponges successfully bind *miR275*, which results in posttranslational
538 knockdown *in vitro*. We detected a significant reduction of *miR275* levels in the midgut of
539 paratransgenic tsetse expressing *miR275* sponges, although we could not reproducibly
540 demonstrate its reduction in the cardia organ. The paratransgenic flies displayed several robust
541 phenotypes that are similar to those of *miR275* depletion via synthetic antagomir-275, including
542 altered blood meal digestion, compromised PM functional integrity, and susceptibility to
543 parasite infection, all of which reflect impaired physiological homeostasis within the gut
544 environment. Our transcriptomic studies further identified new molecular pathways heretofore
545 unknown to be regulated by tsetse *miR275*, including the regulation of abundant secretory
546 proteins functioning in vasoconstriction, platelet aggregation, coagulation, and inflammation or
547 hemostasis. Our study is the first to use paratransgenesis as a strategy to constitutively modify
548 the expression of a microRNA in midgut tissue where the endosymbionts reside. It is efficient,
549 cost effective, and minimally invasive compared to feeding and/or injecting synthetic
550 antagomirs, and as such, this approach serves as an efficacious alternative to investigate
551 microRNA related functions in the tsetse fly gut. This strategy can similarly be employed in any

552 arthropod that houses genetically modifiable commensal gut symbionts that reside within host
553 cells.

554 Several experimental approaches are available to modify miRNA expression *in vivo*.

555 Chemically synthesized, cholesterol bound antisense oligonucleotides (antagomirs) are
556 currently most commonly used. These single stranded oligos bind their complementary
557 endogenous miRNA, thus preventing it from interacting with its target mRNA, which inhibits
558 downstream protein production (74). While synthetic antagomirs interact exclusively with their
559 complimentary miRNA, they must be administered repeatedly and often in large doses for long-
560 term effect, their uptake by cells can be inefficient, and they are difficult to target to specific
561 tissues (75). Transgenic expression of miRNA sponges is another widely used method, which
562 can provide effective and specific inhibition of miRNA seed families (the conserved sequences
563 among miRNAs) (76). This method, which involves the insertion of multiple, tandem antagomirs
564 into the germline, has been successfully used to constitutively deplete miRNA abundance in
565 mosquitoes in a tissue specific manner via the use of tissue specific promoters (18, 77-79).

566 Because all embryonic and larval development occurs within the uterus of female tsetse (80),
567 the generation of transgenic fly lines using traditional germline modification approaches has
568 not been possible. To overcome this impediment, we developed the paratransgenic expression
569 system described herein to constitutively express *miR275* sponges in tsetse's gut.

570 We consistently observed three phenotypes that are associated with modified tsetse
571 midgut physiological homeostasis in our *Gmm*^{3xant-*miR275*} flies compared to *Gmm*^{Scr-275} controls.
572 These phenotypes all correlate with the presentation of a structurally compromised PM, and
573 they are similar to the phenotypes that we observed previously when synthetic antagomir-275

574 was administrated to tsetse. Specifically, we observed that *Gmm*^{3xant-*miR275*} flies presented
575 significantly heavier gut weights, significantly higher survival rates upon challenge with an
576 entomopathogen, and significantly stronger vector competence, as compared to *Gmm*^{Scr-275}
577 controls. Increased midgut weight is indicative of impaired blood meal digestion and/or
578 excretion, and this phenotype was similarly observed following treatment of *Ae. aegypti* (17)
579 and tsetse (11) with synthetic *miR275* antagonir. In hematophagous insects, the PM mediates
580 blood digestion by regulating the flux of digestive enzymes from their site of production in the
581 midgut epithelium into the blood bolus-containing gut lumen (81, 82). Our study also
582 demonstrated that significantly more *Gmm*^{3xant-*miR275*} flies survive in the presence of
583 entomopathogenic *Serratia* than do *Gmm*^{Scr-275} control flies, further indicating that PM
584 functional integrity is compromised in the former group of flies. *Serratia marcescens* strain
585 Db11 is an entomopathogenic bacterium (83) that can kill tsetse when provided in the
586 bloodmeal. Specifically, flies with an intact PM fail to immunologically detect *Serratia*, which
587 allows the bacterium to rapidly proliferate in the gut lumen, translocate into the hemolymph
588 and eventually to kill the tsetse and other insects (7, 10, 11, 83-86). Conversely, when PM
589 structural integrity is compromised, the bacterium is quickly detected by tsetse's midgut
590 epithelium and eliminated by the fly's robust antimicrobial immune response. The *Serratia*
591 infection assay thus serves as a highly sensitive indicator of tsetse's PM structural integrity (7).
592 Lastly, we observed a higher trypanosome infection prevalence in *Gmm*^{3xant-*miR275*} flies
593 compared to *Gmm*^{Scr-275} controls. This outcome is similar to what observed in flies exposed to
594 anti-PM RNAi (dsRNA targeting *pro1*, *pro2* and *chitin synthase*) (7) as well as in flies that were
595 provisioned a blood meal containing a purified trypanosome coat protein (sVSG), which

596 interferes with PM related gene expression in the cardia through the reduction of *miR275* (11).
597 Taken together, our results confirm that interference with *miR275* expression in the cardia and
598 midgut of *Gmm*^{3xant-*miR275*} flies results in the modified gut environment we noted in this study.

599 Herein we repeatedly observed phenotypes that correspond with a depletion of *miR275*
600 expression in tsetse's cardia. However, despite these findings, we were unable to quantify a
601 significant reduction in expression of the microRNA in tsetse's cardia (although we could in the
602 fly's midgut). This outcome may be accounted for by one or several reasons. First, the
603 concentration of paratransgenically expressed *miR275* relative to the concentration of the
604 binding sites may have reduced the inhibitory effect of the miRNA sponges (75). Prior
605 investigations demonstrated that tsetse *miR275* is highly abundant in the cardia compared to
606 the midgut tissues (11). Thus, our depletion effect could have been diluted in the cardia organ
607 where *miR275* are highly abundant. This outcome is further exacerbated by the conspicuously
608 low number of *recSodalis* that colonized cells of tsetse's cardia in comparison to the midgut.
609 More experiments are required to optimize the uptake of *recSodalis* by cells of tsetse's cardia
610 organ. Moreover, qRT-PCR can be an inaccurate method for quantifying the abundance of
611 functional miRNAs, especially in the organ where the miRNAs are highly abundant such as
612 tsetse's cardia. The procedure measures the total amount of miRNAs and doesn't distinguish
613 between functional miRNAs and non-functional ones. Thus, qRT-PCR can quantify the amount
614 of extracellular miRNA released from Trizol-lysed cells, and this represents a physiologically
615 irrelevant population of miRNAs (87). Combined with the robust phenotypic changes and
616 differential expression of blood digestion and PM related genes, we believe that our
617 paratransgenic knockdown was successful at the functional level.

618 Our transcriptomic analyses of cardias and midguts from paratransgenic tsetse revealed
619 several interesting insights into the broader functions of *miR275* that are related to
620 trypanosome infection. First, with regard to the genes that are associated with PM and
621 digestion, midgut GO enrichment analysis indicated that downregulated genes in *Gmm*^{3xant-}
622 *miR275* flies included an enriched population of transcripts that encode proteins involved in
623 ribosome biogenesis and cellular component biogenesis. This suggests that protein synthesis is
624 obstructed in the midguts of *Gmm*^{3xant-*miR275*} flies, which could reflect the compromised PM
625 structure and disrupted digestion we observed in these fly's guts. GO enrichment analysis of
626 upregulated cardia specific genes indicated that genes in *Gmm*^{3xant-*miR275*} flies included a group
627 of enriched transcripts that encode proteins involved in chitin metabolism and chitin binding
628 processes. Chitinase produced by parasites degrades the sand fly and mosquito PM, which
629 promotes *Leishmania* (88) and *Plasmodium* (89) transmission, respectively. The genome of
630 African trypanosomes does not encode a chitinase gene. However, chitinase is a proteinaceous
631 component of tsetse's PM, and infection with trypanosomes induces chitinase expression in the
632 fly's cardia (10, 44, 90) and gut (11). These findings suggest that parasites may facilitate their
633 transmission through the fly by transiently upregulating cardia/gut chitinase expression, thus
634 degrading PM chitin fibrils and reducing the structure's ability to serve as a barrier. We also
635 observed that several genes encoding digestive enzymes were downregulated in the cardia of
636 the *Gmm*^{3xant-*miR275*}. Similarly, *miR275* and digestive enzyme-encoding genes (e.g., those
637 encoding trypsin and trypsin-like proteins) were down-regulated in tsetse's cardia following
638 trypanosome exposure (10, 11). In *Ae. aegypti*, gut-specific depletion of *miR275* results in
639 reduced expression of its target gene *SERCA*, as well as reduced digestive enzyme secretion,

640 disrupted gut microbiota homeostasis and compromised gut actin cytoskeleton integrity.
641 Notably, under these circumstances, protein levels of late trypsin, a late-phase digestive
642 protease in female mosquitoes, are significantly reduced (18). This outcome likely accounts for
643 the altered midgut phenotypes observed in *miR275* knockdown mosquitoes. However, tsetse
644 *SERCA* does not contain orthologous *miR275* binding site motifs, and *SERCA* levels are not
645 differentially expressed in *Gmm*^{3xant-*miR275*} compared to *Gmm*^{Scr-275} flies. These characteristics
646 suggest that the target of tsetse *miR275* may not be *SERCA*, and a currently unknown
647 pathway(s) regulates the secretion of the above-mentioned proteins in tsetse's gut.

648 Notably, in this study the expression of some PM-associated genes was the opposite of
649 what was observed previously when tsetse *miR275* was knocked down via synthetic antagonir-
650 275 (11). In the previous study, expression of *pro1-3* were significantly downregulated in the
651 cardia samples after the *per os* provisioning of either synthetic antagonir-275 or sVSG.
652 Conversely, in this study, *pro1* in the cardia, and *pro2* and *pro3* in the midgut were significantly
653 upregulated in *Gmm*^{3xant-*miR275*} compared to *Gmm*^{Scr-275} flies. However, in a different study of
654 trypanosome-infected tsetse cardia *pro1* is no significant different and *pro2-3* are
655 downregulated, and the downregulation effect of *pro* genes by provisioning sVSG in the cardia
656 is transient (10). This finding suggests that the *pro* genes regulation might be different based on
657 parasite infection status. The observed disparity in *pro* gene expression by *miR275* can be
658 explained by the possibility that the synthetic antagonir produces a one-time reduction in
659 *miR275* expression that causes a different physiological response in the fly compared to that
660 when *miR275* is constitutively suppressed in paratransgenic flies. However, further

661 investigation is required to acquire a more complete understanding of the *miR275* regulatory
662 network and physical fitness.

663 Our transcriptomic results consistently showed *miR275* functions in reducing the
664 expression of secretory enzymes and similarly impairing secretory and digestive pathways.
665 Nineteen saliva-associated proteins were among the putative secretory products that were
666 dramatically reduced in the cardia of the *Gmm*^{3xant-*miR275*} individuals. Interestingly, seventeen of
667 these genes were reduced in trypanosome-infected salivary glands (52, 60, 61), but it remains
668 to be seen if this reduction is also mediated by lower *miR275* levels in infected salivary glands.

669 Previous transcriptomic analyses found that sixteen of these genes were reduced in
670 trypanosome-challenged guts (11). Nine of the saliva protein-encoding transcripts were
671 detected in tsetse's cardia, but only four were differentially expressed upon trypanosome
672 infection (10). In addition to being major constituents of saliva, *Adgf*, *TTI* and *5'Nuc* are
673 expressed in tsetse's cardia and gut tissues, suggesting that these molecules may also play a
674 role in digestive processes (59, 60, 63-65). The reduction of these saliva-associated
675 anticoagulants in infected flies causes increased probing and biting behaviors, which in turn
676 increases the transmission potential of the parasite to multiple hosts (60). The significant
677 reduction in expression of genes in the *Adgf* family was also very interesting. *Adgf* is a secreted
678 enzyme that converts extracellular adenosine into inosine by deamination and is important in
679 anti-inflammation, tissue damage and resistance to bacterial infection in *Drosophila* (91-93). A
680 *Adgf* is expressed by immune cells to regulate the metabolic switch during bacterial infection in
681 *Drosophila*, and the downregulation of *Adgf* increases extracellular adenosine and enhances
682 resistance to bacterial infection (91). The loss of *Adgf* can induces intestinal stem cell

683 proliferation in *Drosophila* (93). As evidenced by reduced *Adgf* gene expressions in
684 trypanosome-challenged tsetse guts, the downregulation of *Adgf* genes might be triggered by
685 initial infection of trypanosomes to release anti-inflammatory response and/or to repair any
686 damaged tissues. Interestingly, Matetovici *et al* (2016) noted significantly reduced expression of
687 genes that encode saliva-associated products in the SGs of flies that house trypanosomes in
688 their midgut but not yet in their SGs. This finding is suggestive of a molecular dialogue between
689 the organs, and a possible anticipatory response of the SG environment prior to the parasites
690 infecting the tissue, which may be mediated by *miR275* levels in these tissues. Given that these
691 genes encode secreted proteins, their strong reduction in paratransgenic tsetse further
692 supports the role of *miR275* in trypanosome infection, possibly through regulation of secretory
693 pathways.

694 Arthropod-borne diseases impose a debilitating global public health burden. Due to the
695 lack of effective vaccines capable of preventing the majority of these diseases, and the
696 increasing resistance of vector arthropods to pesticides, alternative approaches for disease
697 control are urgently needed. Paratransgenic systems have been applied in efforts to reduce
698 vector competence in mosquitoes (30, 31, 94, 95), kissing bugs (96, 97), sand flies (98) and
699 tsetse flies (25-27, 99). This technology has many benefits, including the absence of a reliance
700 on inefficient germline modification procedures (88), and the fact that modified symbionts
701 exert no fitness cost on their insect hosts (24) and can potentially spread through wild vector
702 populations via vertical transmission (100). Additionally, paratransgenically expressed
703 microRNAs costs significantly less than do their synthetically produced counterparts. Our study
704 is the first to use this system to explore the function of an arthropod vector microRNA in

705 relation to disease transmission processes. This system can be easily applied to study the
706 function of other tsetse miRNAs and for future research aimed at experimentally interfering
707 with the physiological homeostasis of tsetse's midgut environment with the intent of
708 interrupting trypanosome transmission through the fly. This study also expanded our
709 knowledge of the relationship between tsetse *miR275* and the regulation of key physiological
710 processes such as blood digestion, PM integrity, and gut environment homeostasis in tsetse.
711 Our transcriptomic data revealed functions regulated by *miR275* affecting tsetse's secretory
712 pathways. These findings provide a foundation for discovering the target of tsetse *miR275* in
713 future studies.

714 **Acknowledgements**

715 This work was made possible with funding to Serap Aksoy from NIH/NIAID (R01AI139525), the

716 Li Foundation and Ambrose Monell Foundation.

717 **Reference cited**

718 1. Simarro PP, Cecchi G, Franco JR, Paone M, Diarra A, Ruiz-Postigo JA, et al. Estimating and
719 mapping the population at risk of sleeping sickness. *PLoS Neglected Tropical Diseases*.
720 2012;6(10):e1859.

721 2. Aksoy S, Gibson WC, Lehane MJ. Interactions between tsetse and trypanosomes with
722 implications for the control of trypanosomiasis. *Advances in Parasitology*. 2003;53:1-83.

723 3. Beschin A, Van Den Abbeele J, De Baetselier P, Pays E. African trypanosome control in
724 the insect vector and mammalian host. *Trends Parasitol*. 2014;30(11):538-47.

725 4. Sutherland CS, Stone CM, Steinmann P, Tanner M, Tediosi F. Seeing beyond 2020: an
726 economic evaluation of contemporary and emerging strategies for elimination of *Trypanosoma*
727 *brucei gambiense*. *The Lancet Global Health*. 2017;5(1):e69-79.

728 5. Abbeele JVD, Claes Y, Bockstaale Dv, D DLR, Coosemans M. *Trypanosoma brucei* spp.
729 development in the tsetse fly: characterization of the post-mesocyclic stages in the foregut and
730 proboscis. *Parasitology*. 1999;118(Pt 5):469-78.

731 6. Gibson W, Bailey M. The development of *Trypanosoma brucei* within the tsetse fly
732 midgut observed using green fluorescent trypanosomes. *Kinetoplastid Biology and Disease*.
733 2003;2(1).

734 7. Weiss BL, Savage AF, Griffith BC, Wu Y, Aksoy S. The peritrophic matrix mediates
735 differential infection outcomes in the tsetse fly gut following challenge with commensal,
736 pathogenic and parasitic microbes. *Journal of Immunology*. 2014;193(2):773-82.

737 8. Weiss BL, Wang J, Maltz MA, Wu Y, Aksoy S. Trypanosome infection establishment in the
738 tsetse fly gut is influenced by microbiome-regulated host immune barriers. *PLoS Pathogens*.
739 2013;9(4):e1003318.

740 9. Rose C, Casas-Sanchez A, Dyer NA, Solorzano C, Beckett AJ, Middlehurst B, et al.
741 *Trypanosoma brucei* colonizes the tsetse gut via an immature peritrophic matrix in the
742 proventriculus. *Nat Microbiol*. 2020;5(7):909-16.

743 10. Vigneron A, Aksoy E, Weiss BL, Bing X, Zhao X, Awuoch EO, et al. A fine-tuned vector-
744 parasite dialogue in tsetse's cardia determines peritrophic matrix integrity and trypanosome
745 transmission success. *PLoS Pathogens*. 2018;14(4):e1006972.

746 11. Aksoy E, Vigneron A, Bing X, Zhao X, O'Neill M, Wu Y-n, et al. Mammalian African
747 trypanosome VSG coat enhances tsetse's vector competence. *PNAS*. 2016;113(25):6961-6.

748 12. Bartel DP. MicroRNAs: Target Recognition and Regulatory Functions. *Cell*.
749 2009;136(2):215-33.

750 13. Fabian MR, Sonenberg N, Filipowicz W. Regulation of mRNA translation and stability by
751 microRNAs. *Annu Rev Biochem*. 2010;79:351-79.

752 14. Hussain M, Walker T, O'Neill SL, Asgari S. Blood meal induced microRNA regulates
753 development and immune associated genes in the Dengue mosquito vector, *Aedes aegypti*.
754 *Insect Biochemistry and Molecular Biology*. 2013;43(2):146-52.

755 15. Dharap A, Pokrzywa C, Murali S, Pandi G, Vemuganti R. MicroRNA miR-324-3p Induces
756 Promoter-Mediated Expression of RelA Gene. *PLOS ONE*. 2013;8(11):e79467.

757 16. Truesdell SS, Mortensen RD, Seo M, Schroeder JC, Lee JH, LeTonqueze O, et al.
758 MicroRNA-mediated mRNA Translation Activation in Quiescent Cells and Oocytes Involves
759 Recruitment of a Nuclear microRNP. *Scientific Reports*. 2012;2(1):842.

760 17. Bryant B, Macdonald W, Raikhel AS. microRNA miR-275 is indispensable for blood
761 digestion and egg development in the mosquito *Aedes aegypti*. *PNAS*. 2010;107(52):22391–8.

762 18. Zhao B, Lucas KJ, Saha TT, Ha J, Ling L, Kokoza VA, et al. MicroRNA-275 targets
763 sarco/endoplasmic reticulum Ca²⁺ adenosine triphosphatase (SERCA) to control key functions
764 in the mosquito gut. *PLoS Genetics*. 2017;13(8):e1006943.

765 19. Wang J, Weiss BL, Aksoy S. Tsetse fly microbiota: form and function. *Frontiers in Cellular
766 and Infection Microbiology*. 2013;3(69).

767 20. Doudoumis V, Blow F, Saridaki A, Augustinos A, Dyer NA, Goodhead I, et al. Challenging
768 the Wigglesworthia, Sodalis, Wolbachia symbiosis dogma in tsetse flies: Spiroplasma is present
769 in both laboratory and natural populations. *Scientific Reports*. 2017;7(1):4699.

770 21. Balmand S, Lohs C, Aksoy S, Heddi A. Tissue distribution and transmission routes for the
771 tsetse fly endosymbionts. *Journal of Invertebrate Pathology*. 2013;112(Supplement 1):S116–
772 S22.

773 22. Weiss BL, Wu Y, Schwank JJ, Tolwinski NS, Aksoy S. An insect symbiosis is influenced by
774 bacterium-specific polymorphisms in outer-membrane protein A. *Proceedings of the National
775 Academy of Sciences*. 2008;105(39):15088–93.

776 23. Maltz MA, Weiss BL, O'Neill M, Wu Y, Aksoy S. OmpA-mediated biofilm formation is
777 essential for the commensal bacterium *Sodalis glossinidius* to colonize the tsetse fly gut.
778 *Applied and Environmental Microbiology*. 2012;78(21):7760–8.

779 24. Weiss BL, Mouchotte R, Rio RVM, Wu Y-n, Wu Z, Heddi A, et al. Interspecific Transfer of
780 Bacterial Endosymbionts between Tsetse Fly Species: Infection Establishment and Effect on
781 Host Fitness. *Applied and Environmental Microbiology*. 2006;72(11):7013–21.

782 25. De Vooght L, Caljon G, Stijlemans B, Baetselier PD, Coosemans M, Abbeele JVD.
783 Expression and extracellular release of a functional anti-trypanosome Nanobody® in *Sodalis
784 glossinidius*, a bacterial symbiont of the tsetse fly. *Microbial Cell Factories*. 2012;11:23.

785 26. De Vooght L, Caljon G, Ridder KD, Abbeele JVD. Delivery of a functional anti-
786 trypanosome Nanobody in different tsetse fly tissues via a bacterial symbiont, *Sodalis
787 glossinidius*. *Microbial Cell Factories*. 2014;13:156.

788 27. De Vooght L, Keer SV, Abbeele JVD. Towards improving tsetse fly paratransgenesis:
789 stable colonization of *Glossina morsitans morsitans* with genetically modified *Sodalis*. *BMC
790 Microbiology*. 2018;18(Supplemental 1):31–8.

791 28. Taracena ML, Oliveira PL, Almendares O, Umaña C, Lowenberger C, Dotson EM, et al.
792 Genetically modifying the insect gut microbiota to control Chagas disease vectors through
793 systemic RNAi. *PLoS neglected tropical diseases*. 2015;9(2):e0003358–e.

794 29. Whitten MMA, Facey PD, Sol RD, Fernández-Martínez LT, Evans MC, Mitchell JJ, et al.
795 Symbiont-mediated RNA interference in insects. *Proceedings of the Royal Society B: Biological
796 Sciences*. 2016;283(1825):20160042.

797 30. Ren X, Hoiczyk E, Rasgon JL. Viral paratransgenesis in the malaria vector *Anopheles
798 gambiae*. *Plos pathogens*. 2008;4(8):e1000135.

799 31. Asgari M, Ilbeigikhamehnejad M, Rismani E, Dinparast Djadid N, Raz A. Molecular
800 characterization of RNase III protein of *Asaia* sp. for developing a robust RNAi-based
801 paratransgenesis tool to affect the sexual life-cycle of *Plasmodium* or *Anopheles* fitness.
802 *Parasites & Vectors*. 2020;13(1):42.

803 32. Qi LS, Larson MH, Gilbert LA, Doudna JA, Weissman JS, Arkin AP, et al. Repurposing
804 CRISPR as an RNA-guided platform for sequence-specific control of gene expression. *Cell*.
805 2013;152(5):1173-83.

806 33. Hrusa G, Farmer W, Weiss BL, Applebaum T, Roma JS, Szeto L, et al. TonB-Dependent
807 Heme Iron Acquisition in the Tsetse Fly Symbiont *Sodalis glossinidius*. *Applied and*
808 *Environmental Microbiology*. 2015;81(8):2900-9.

809 34. A.Elsinghorst E. Measurement of invasion by gentamicin resistance. *Methods in*
810 *Enzymology*. 2361994. p. 405-20.

811 35. Chomczynski P, Sacchi N. Single-step method of RNA isolation by acid guanidinium
812 thiocyanate-phenol-chloroform extraction. *Analytical Biochemistry*. 1987;162(1):156-9.

813 36. Initiative IGG. Genome sequence of the tsetse fly (*Glossina morsitans*): Vector of African
814 trypanosomiasis. *Science*. 2014;344(6182):380-6.

815 37. Kim D, Langmead B, Salzberg SL. HISAT: a fast spliced aligner with low memory
816 requirements. *Nature Methods*. 2015;12(4):357-60.

817 38. Kim D, Paggi JM, Park C, Bennett C, Salzberg SL. Graph-based genome alignment and
818 genotyping with HISAT2 and HISAT-genotype. *Nature Biotechnology*. 2019;37(8):907-15.

819 39. Anders S, Pyl PT, Huber W. HTSeq—a Python framework to work with high-throughput
820 sequencing data. *Bioinformatics*. 2014;31(2):166-9.

821 40. Chen Y, McCarthy D, Ritchie M, Robinson M, Smyth G. edgeR: differential expression
822 analysis of digital gene expression data User's Guide 2019 [Available from:
823 <http://www.bioconductor.org/packages/release/bioc/vignettes/edgeR/inst/doc/edgeRUsersGuide.pdf>].

825 41. Supek F, Bosnjak M, Skunca N, Smuc T. REVIGO summarizes and visualizes long lists of
826 gene ontology terms. *PLoS One*. 2011;6(7):e21800.

827 42. Haines LR. Examining the tsetse teneral phenomenon and permissiveness to
828 trypanosome infection. *Front Cell Infect Microbiol*. 2013;3:84.

829 43. Macleod ET, MAUDLIN I, Darby AC, Welburn SC. Antioxidants promote establishment of
830 trypanosome infections in tsetse. *Parasitology*. 2007;134(6):827-31.

831 44. Rose C, Belmonte R, Armstrong SD, Molyneux G, Haines LR, Lehane MJ, et al. An
832 Investigation into the Protein Composition of the Teneral *Glossina morsitans morsitans*
833 Peritrophic Matrix. *PLoS Neglected Tropical Diseases*. 2014;8(4):e2691.

834 45. Haines LR, Jackson AM, Lehane MJ, Thomas JM, Yamaguchi AY, Haddow JD, et al.
835 Increased expression of unusual EP repeat-containing proteins in the midgut of the tsetse fly
836 (*Glossina*) after bacterial challenge. *Insect Biochemistry and Molecular Biology*. 2005;35(5):413-
837 23.

838 46. Haines LR, Lehane SM, Pearson TW, Lehane MJ. Tsetse EP Protein Protects the Fly
839 Midgut from Trypanosome Establishment. *PLoS pathogens*. 2010;6(3):e1000793.

840 47. Hegedus D, Erlandson M, Gillott C, Toprak U. New insights into peritrophic matrix
841 synthesis, architecture, and function. *Annual Review of Entomology*. 2009;54:285-302.

842 48. Merzendorfer H, Zimoch L. Chitin metabolism in insects: structure, function and
843 regulation of chitin synthases and chitinases. *Journal of Experimental Biology*.
844 2003;206(24):4393.

845 49. Hamidou Soumana I, Tchicaya B, Rialle S, Parrinello H, Geiger A. Comparative Genomics
846 of *Glossina palpalis gambiensis* and *G. morsitans morsitans* to Reveal Gene Orthologs Involved
847 in Infection by *Trypanosoma brucei gambiense*. *Frontiers in microbiology*. 2017;8:540-.

848 50. Feyereisen R. 8 - Insect CYP Genes and P450 Enzymes. In: Gilbert LI, editor. *Insect*
849 *Molecular Biology and Biochemistry*. San Diego: Academic Press; 2012. p. 236-316.

850 51. Félix RC, Müller P, Ribeiro V, Ranson H, Silveira H. Plasmodium infection alters
851 *Anopheles gambiae* detoxification gene expression. *BMC Genomics*. 2010;11:312.

852 52. Matetovici I, Caljon G, Abbeele JVD. Tsetse fly tolerance to *T. brucei* infection:
853 transcriptome analysis of trypanosome- associated changes in the tsetse fly salivary gland. *BMC*
854 *Genomics*. 2016;17.

855 53. Sterkel M, Oliveira JHM, Bottino-Rojas V, Paiva-Silva GO, Oliveira PL. The Dose Makes
856 the Poison: Nutritional Overload Determines the Life Traits of Blood-Feeding Arthropods.
857 *Trends in Parasitology*. 2017;33(8):633-44.

858 54. Pascoa V, Oliveira PL, Dansa-Petretski M, Silva JR, Alvarenga PH, Jacobs-Lorena M, et al.
859 *Aedes aegypti* peritrophic matrix and its interaction with heme during blood digestion. *Insect*
860 *Biochem Mol Biol*. 2002;32(5):517-23.

861 55. Gerke V, Moss SE. Annexins: From Structure to Function. *Physiological Reviews*.
862 2002;82(2):331-71.

863 56. Kotsyfakis M, Ehret-Sabatier L, Siden-Kiamos I, Mendoza J, Sinden RE, Louis C.
864 *Plasmodium berghei* ookinetes bind to *Anopheles gambiae* and *Drosophila melanogaster*
865 annexins. *Molecular Microbiology*. 2005;57(1):171-9.

866 57. Güiza J, Barría I, Sáez JC, Vega JL. Innexins: Expression, Regulation, and Functions.
867 *Frontiers in physiology*. 2018;9:1414-.

868 58. Bauer R, Lehmann C, Fuss B, Eckardt F, Hoch M. The *Drosophila* gap junction channel
869 gene innixin 2 controls foregut development in response to Wingless signalling. *J Cell Sci*.
870 2002;115(Pt 9):1859-67.

871 59. Li S, Aksoy S. A family of genes with growth factor and adenosine deaminase similarity
872 are preferentially expressed in the salivary glands of *Glossina m. morsitans*. *Gene*. 2000;252(1-
873 2):83-93.

874 60. Van Den Abbeele J, Caljon G, De Ridder K, De Baetselier P, Coosemans M. *Trypanosoma*
875 *brucei* modifies the tsetse salivary composition, altering the fly feeding behavior that favors
876 parasite transmission. *PLoS Pathog*. 2010;6(6):e1000926.

877 61. Telleria EL, Benoit JB, Zhao X, Savage AF, Regmi S, Alves e Silva TL, et al. Insights into the
878 trypanosome-host interactions revealed through transcriptomic analysis of parasitized tsetse fly
879 salivary glands. *PLoS Negl Trop Dis*. 2014;8(4):e2649.

880 62. Alves-Silva J, Ribeiro JM, Abbeele JVD, Attardo G, Hao Z, Haines LR, et al. An insight into
881 the sialome of *Glossina morsitans morsitans*. *BMC Genomics*. 2010;11.

882 63. Caljon G, De Ridder K, De Baetselier P, Coosemans M, Van Den Abbeele J. Identification
883 of a tsetse fly salivary protein with dual inhibitory action on human platelet aggregation. *PLoS*
884 *One*. 2010;5(3):e9671.

885 64. Cappello M, Bergum PW, Vlasuk GP, Fumidge BA, Pritchard DI, Aksoy S. Isolation and
886 Characterization of the Tsetse Thrombin Inhibitor: A Potent Antithrombotic Peptide from the
887 Saliva of *Glossina morsitans morsitans*. *The American Journal of Tropical Medicine and Hygiene*.
888 1996;54(5):475-80.

889 65. Cappello M, Li S, Chen X, Li CB, Harrison L, Narashimhan S, et al. Tsetse thrombin
890 inhibitor: bloodmeal-induced expression of an anticoagulant in salivary glands and gut tissue of
891 *Glossina morsitans morsitans*. Proceedings of the National Academy of Sciences of the United
892 States of America. 1998;95(24):14290-5.

893 66. Caljon G, Broos K, De Goeijse I, De Ridder K, Sternberg JM, Coosemans M, et al.
894 Identification of a functional Antigen5-related allergen in the saliva of a blood feeding insect,
895 the tsetse fly. Insect Biochemistry and Molecular Biology. 2009;39(5):332-41.

896 67. Zhao Y, Li Z, Gu X, Su Y, Liu L. Imaginal Disc Growth Factor 6 (Idgf6) Is Involved in Larval
897 and Adult Wing Development in *Bactrocera correcta* (Bezzi) (Diptera: Tephritidae). Front Genet.
898 2020;11:451-.

899 68. Swarup S, Verheyen EM. Wnt/Wingless signaling in *Drosophila*. Cold Spring Harb
900 Perspect Biol. 2012;4(6):a007930.

901 69. Cohen E. Chapter 2 - Chitin Biochemistry: Synthesis, Hydrolysis and Inhibition. In: Casas
902 J, Simpson SJ, editors. Advances in Insect Physiology. 38: Academic Press; 2010. p. 5-74.

903 70. Feyereisen R. Evolution of insect P450. Biochemical Society Transactions.
904 2006;34(6):1252-5.

905 71. Ribeiro JMC. A catalogue of *Anopheles gambiae* transcripts significantly more or less
906 expressed following a blood meal. Insect Biochemistry and Molecular Biology. 2003;33(9):865-
907 82.

908 72. Bogdan C. Nitric oxide and the immune response. Nat Immunol. 2001;2(10):907-16.

909 73. Hao Z, Kasumba I, Aksoy S. Proventriculus (cardia) plays a crucial role in immunity in
910 tsetse fly (Diptera: Glossinidae). Insect Biochem Mol Biol. 2003;33(11):1155-64.

911 74. Horwich MD, Zamore PD. Design and delivery of antisense oligonucleotides to block
912 microRNA function in cultured *Drosophila* and human cells. Nature Protocols. 2008;3:1537-49.

913 75. Ebert MS, Sharp PA. MicroRNA sponges: Progress and possibilities. RNA.
914 2010;16(11):2043-50.

915 76. Ebert MS, Neilson JR, Sharp PA. MicroRNA sponges: competitive inhibitors of small RNAs
916 in mammalian cells. Nature methods. 2007;4(9):721-6.

917 77. Lucas KJ, Roy S, Ha J, Gervaise AL, Kokko VA, Raikhel AS. MicroRNA-8 targets the
918 Wingless signaling pathway in the female mosquito fat body to regulate reproductive
919 processes. PNAS. 2015;112(5):1440-5.

920 78. Zhang X, Aksoy E, Girke T, Raikhel AS, Karginov FV. Transcriptome-wide microRNA and
921 target dynamics in the fat body during the gonadotrophic cycle of *Aedes aegypti*. PNAS.
922 2017;114(10):E1895-E903.

923 79. Dong S, Fu X, Dong Y, Simões ML, Zhu J, Dimopoulos G. Broad spectrum
924 immunomodulatory effects of *Anopheles gambiae* microRNAs and their use for transgenic
925 suppression of *Plasmodium*. PLOS Pathogens. 2020;16(4):e1008453.

926 80. Benoit JB, Attardo GM, Baumann AA, Michalkova V, Aksoy S. Adenotrophic viviparity in
927 tsetse flies: potential for population control and as an insect model for lactation. Annual review
928 of entomology. 2015;60:351-71.

929 81. Kato N, Mueller CR, Fuchs JF, McElroy K, Wessely V, Higgs S, et al. Evaluation of the
930 function of a type I peritrophic matrix as a physical barrier for midgut epithelium invasion by
931 mosquito-borne pathogens in *Aedes aegypti*. Vector Borne and Zoonotic Diseases.
932 2008;8(5):701-12.

933 82. Baia-da-Silva DC, Alvarez LCS, Lizcano OV, Costa FTM, Lopes SCP, Orfanó AS, et al. The
934 role of the peritrophic matrix and red blood cell concentration in *Plasmodium vivax* infection of
935 *Anopheles aquasalis*. *Parasites & Vectors*. 2018;11(1):148.

936 83. Nehme NT, Liégeois S, Kele B, Giammarinaro P, Pradel E, Hoffmann JA, et al. A model of
937 bacterial intestinal infections in *Drosophila melanogaster*. *PLoS Pathog*. 2007;3(11):e173.

938 84. Weiss BL, Maltz MA, Vigneron A, Wu Y, Walter KS, O'Neil MB, et al. Colonization of the
939 tsetse fly midgut with commensal *Kosakonia cowanii* *Zambiae* inhibits trypanosome infection
940 establishment. *PLoS Pathogens*. 2019;15(2):e1007470.

941 85. Muhammad A, Habineza P, Ji T, Hou Y, Shi Z. Intestinal Microbiota Confer Protection by
942 Priming the Immune System of Red Palm Weevil *Rhynchophorus ferrugineus* Olivier
943 (Coleoptera: Dryophthoridae). *Frontiers in Physiology*. 2019;10(1303).

944 86. Kuraishi T, Binggeli O, Opota O, Buchon N, Lemaitre B. Genetic evidence for a protective
945 role of the peritrophic matrix against intestinal bacterial infection in *Drosophila*
946 *melanogaster*. *Proceedings of the National Academy of Sciences*. 2011;108(38):15966-
947 71.

948 87. Thomson DW, Bracken CP, Szubert JM, Goodall GJ. On measuring miRNAs after transient
949 transfection of mimics or antisense inhibitors. *PLoS One*. 2013;8(1):e55214.

950 88. Coutinho-Abreu IV, Sharma NK, Robles-Murguia M, Ramalho-Ortigao M. Targeting the
951 Midgut Secreted PpChit1 Reduces *Leishmania* major Development in Its Natural Vector, the
952 Sand Fly *Phlebotomus papatasii*. *PLOS Neglected Tropical Diseases*. 2010;4(11):e901.

953 89. Li F, Patra KP, Vinetz JM. An Anti-Chitinase Malaria Transmission-Blocking Single-Chain
954 Antibody as an Effector Molecule for Creating a *Plasmodium falciparum*-Refractory Mosquito.
955 *The Journal of Infectious Diseases*. 2005;192(5):878-87.

956 90. Dyer NA, Rose C, Ejeh NO, Acosta-Serrano A. Flying tryps: survival and maturation of
957 trypanosomes in tsetse flies. *Trends in Parasitology*. 2013;29(4):188-96.

958 91. Bajgar A, Dolezal T. Extracellular adenosine modulates host-pathogen interactions
959 through regulation of systemic metabolism during immune response in *Drosophila*. *PLOS*
960 *Pathogens*. 2018;14(4):e1007022.

961 92. Novakova M, Dolezal T. Expression of *Drosophila* Adenosine Deaminase in Immune Cells
962 during Inflammatory Response. *PLOS ONE*. 2011;6(3):e17741.

963 93. Xu C, Franklin BJ, Tang H-W, Regimbald-Dumas Y, Hu Y, Ramos J, et al. An in vivo RNAi
964 screen uncovers the role of AdoR signaling and adenosine deaminase in controlling intestinal
965 stem cell activity. *Proceedings of the National Academy of Sciences*. 2019;117:464 - 71.

966 94. Wang S, Jacobs-Lorena M. Chapter 13 - Paratransgenesis Applications: Fighting Malaria
967 With Engineered Mosquito Symbiotic Bacteria. In: Wikel SK, Aksoy S, Dimopoulos G, editors.
968 *Arthropod Vector: Controller of Disease Transmission, Volume 1*: Academic Press; 2017. p. 219-
969 34.

970 95. Shane JL, Grogan CL, Cwalina C, Lampe DJ. Blood meal-induced inhibition of vector-
971 borne disease by transgenic microbiota. *Nature Communications*. 2018;9(1):4127.

972 96. Durvasula RV, Gumbs A, Panackal A, Kruglov O, Taneja J, Kang AS, et al. Expression of a
973 functional antibody fragment in the gut of *Rhodnius prolixus* via transgenic bacterial symbiont
974 *Rhodococcus rhodnii*. *Medical and Veterinary Entomology*. 1999;13(2):115-9.

975 97. Beard CB, Cordon-Rosales C, Durvasula RV. Bacterial symbionts of the Triatominae and
976 their potential use in control of Chagas disease transmission. *Annual Review of Entomology*.
977 2002;47:123-41.

978 98. Hurwitz I, Hillesland H, Fieck A, Das P, Durvasula R. The paratransgenic sand fly: A
979 platform for control of *Leishmania* transmission. *Parasites & Vectors*. 2011;4.

980 99. Aksoy S, Weiss B, Attardo G. Paratransgenesis applied for control of tsetse transmitted
981 sleeping sickness. *Adv Exp Med Biol*. 2008;627:35-48.

982 100. Cheng Q, Aksoy S. Tissue tropism, transmission and expression of foreign genes in vivo
983 in midgut symbionts of tsetse flies. *Insect Molecular Biology*. 1999;8(1):125-32.

984

985

986 **Figure 1. The successful development of paratransgenic expression system.**

987 (A) *recSodalis* plasmid construct. Three tandem antagonir-275 repeats (3xant-*miR275*, in
988 green) that are complementary to the tsetse *miR275* mature sequence were cloned into
989 plasmid pgRNA. Each repeat is separated by a 3-nucleotide linker sequence. 3xant-*miR275*,
990 and a similarly engineered construct that encodes a scrambled antagonir-275 (Scr-275),
991 were electroporated into *Sodalis*^{WT} to generate strains designated *Sgm*^{3xant-*miR275*} and *Sgm*<sup>Scr-
992 275</sup>, respectively.

993 (B) Quantification of *Sgm*^{3xant-*miR275*} within cells of tsetse's cardia (black) and midgut (grey) via
994 gentamicin exclusion assay. Each dot represents one tsetse organ (n=5). A student's t-test
995 was used to determine statistical significance.

996 (C) Dual luciferase reporter assay. Each dot represents the average of normalized luciferase
997 signal (*Renilla*/*Firefly* ratio) \pm SEM of each experiment. The 3xant-*miR275* construct was
998 cloned into the psiCheck-2 plasmid containing two luciferase reporter genes, *Renilla*
999 (reporter) and *Firefly* (internal control). The luciferase activity is measured by the *Renilla*
1000 signal normalized to the *Firefly* signal. Three different experiments were performed to test
1001 the binding efficacy between 3xant-*miR275* and 1) synthetic miR275 mimic, 2) synthetic
1002 AllStars Negative Control, and 3) psiCheck plasmid without adding any miRNA. Three
1003 biological replicates (with 3 technical replicates each) per experiment were used.
1004 Bonferroni's multiple comparison tests were used to determine statistical significance.

1005 (D) *miR275* expression level in the midgut of paratransgenic *Gmm*^{3xant-*miR275*} versus *Gmm*^{Scr-275}
1006 flies. Each dot represents 5 individual midguts. A student's t-test was used to determine
1007 statistical significance.

1008 (E) *miR275* expression in the cardia of *Gmm*^{3xant-*miR275*} versus *Gmm*^{Scr-275} flies. Each dot
1009 represents 5 individual cardia. A student's t-test was used for statistical analysis.

1010

1011 **Figure 2. Gut physiological homeostasis is compromised in *Gmm*^{3xant-*miR275*}.**

1012 (A) Tsetse gut weights. The gut weights were measured 24 h after the last blood meal. Each dot
1013 represents an individual fly gut. Mann-Whitney test was used for statistical analysis.

1014 (B) *Serratia* infection assay. A total of 4 biological replicates (n=25 flies per replicate) were
1015 used. Gehan-Breslow-Wilcoxon test was used to determine statistical significance.

1016 (C) Trypanosome midgut infection prevalence. Four biological replicates (n=20 flies per
1017 replicate) were used. Generalized linear model (GLM) with binomial distribution was used
1018 to determine statistical significance.

1019

1020 **Figure 3. Overviews of transcriptome profiles in *Gmm*^{3xant-*miR275*} compared to *Gmm*^{Scr-275} flies.**

1021 (A) cardia and (B) midgut transcriptome profile overview. Left panel: MDS plots display the
1022 overall gene expression patterns among the samples and between the treatments.
1023 Right panel: Venn diagrams show the number of downregulated (blue), upregulated (red) and
1024 not significantly different (white) genes in (A) cardia and (B) midgut. Genes were considered DE
1025 if they exhibited an FDR value <0.05.

1026

1027 **Figure 4. GO enrichment analysis of the paratransgenic flies *Gmm*^{3xant-*miR275*} vs. *Gmm*^{Scr-275}.**

1028 (A) cardia and (B) midgut tissues GO enrichment analyses. Three GO term categories were
1029 used: biological process (yellow), cellular component (green), and molecular function (pink).

1030 The GO terms were considered significant (Bonferroni score < 0.05) using VectorBase built-in
1031 GO enrichment analysis web tool. Redundant GO terms were removed by REVIGO (0.5). The
1032 number of genes in our dataset/ the total number of genes that are associated to each
1033 individual GO term, are marked within parentheses next to each GO term description.

1034

1035 **Figure 5. Heat map representation of DE genes in different functional groups (A-D) in**
1036 **paratransgenic cardia *Gmm*^{3xant-miR275} vs. *Gmm*^{Scr-275}.**

1037 (A) PM and digestion associated, (B) heme binding and detoxification, (C) transporter
1038 associated, and (D) saliva associated. Heat maps were generated by plotting the read counts in
1039 treatment (3xant-miR275) and control (Scr-275) samples. Colors display normalized gene
1040 expression values from low (blue) to high (red). * indicates the unknown gene product's
1041 orthologue in *Drosophila melanogaster* (*Dm*) and/or *Musca domestica* (*Md*).

1042

1043 **Figure 6. Heat map representation of DE genes in different functional groups (A-C) in the**
1044 **midgut of *Gmm*^{3xant-miR275} and *Gmm*^{Scr-275} flies.**

1045 (A) PM and digestion associated, (B) transporter associated, and (C) heme binding and
1046 oxidative response associated. Heat maps were generated by plotting the read counts in in
1047 treatment (3xant-miR275) and control (Scr-275) samples. Colors display normalized gene
1048 expression values from low (blue) to high (red). * indicates the unknown gene product's
1049 orthologue in *Drosophila melanogaster* (*Dm*) and/or *Musca domestica* (*Md*).

1050

1051 **Figure 7. The paratransgenic system is gut tissue specific.**

1052 (A) *miR275*, (B) *Adgf3*, (C) *Adgf5* and (D) *SGP1* expression levels in the salivary glands (SGs) of
1053 *Gmm*^{3xant-*miR275*} versus *Gmm*^{Scr-275} flies. Each dot represents 10 individual SGs. Student's t-test
1054 was used to determine statistical significance.

1055

1056

1057 **Supporting information**

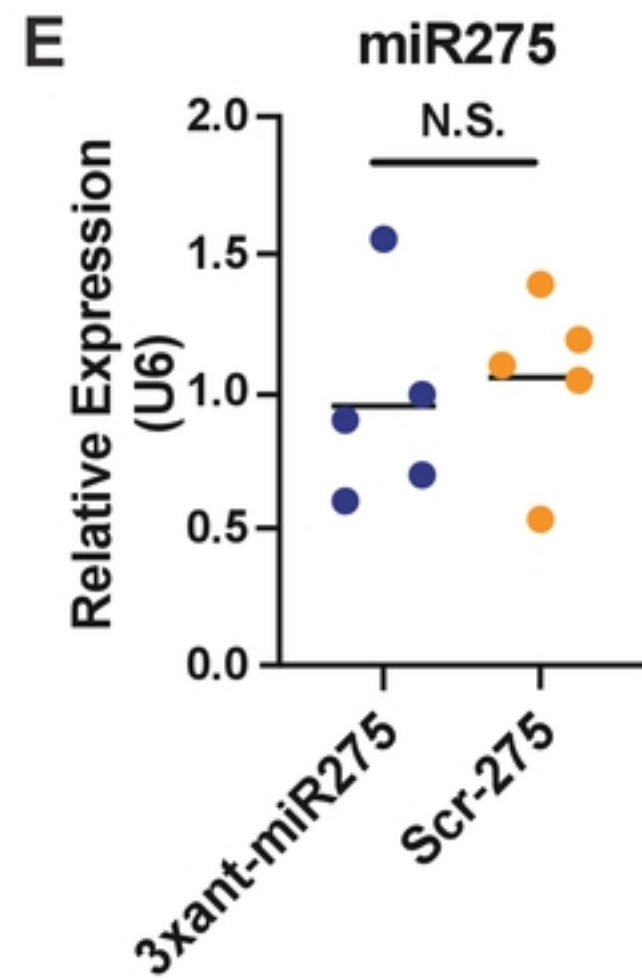
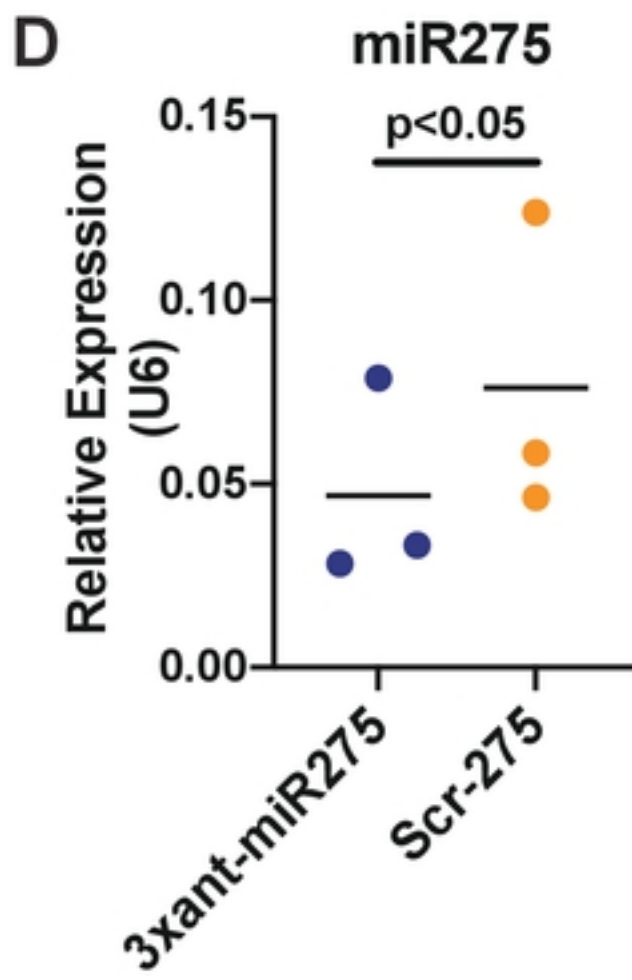
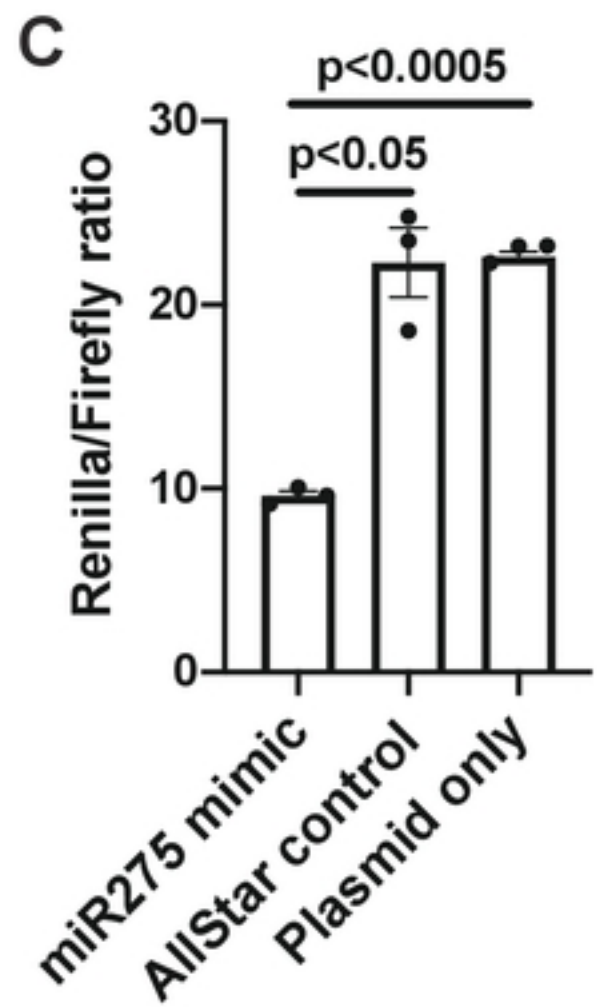
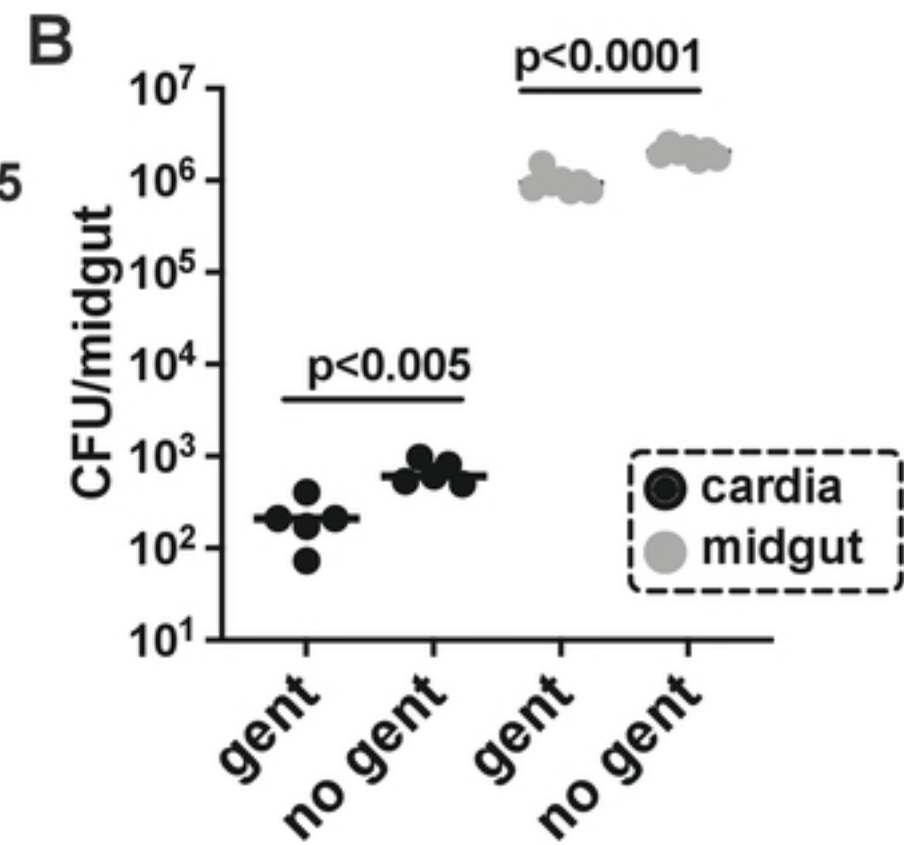
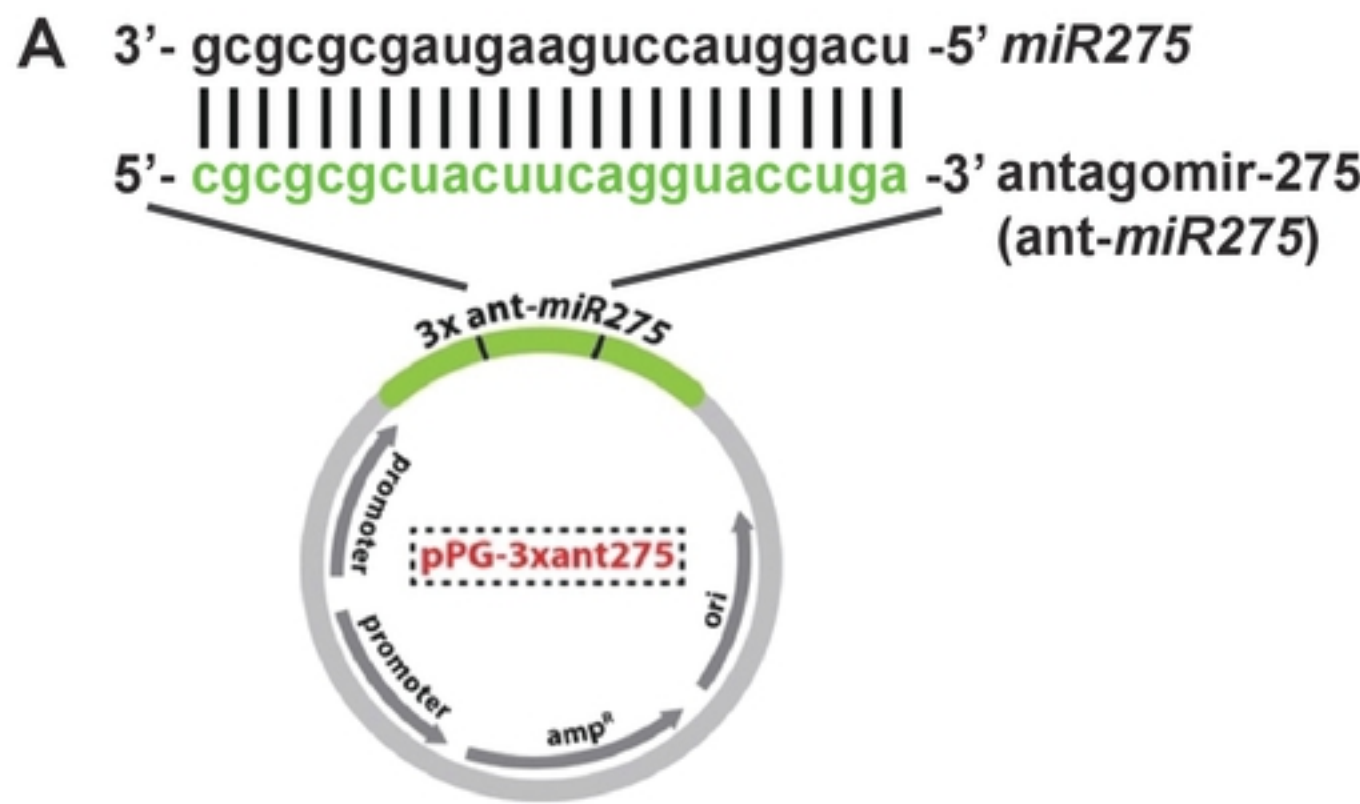
1058 **Table S1. qPCR primer list.**

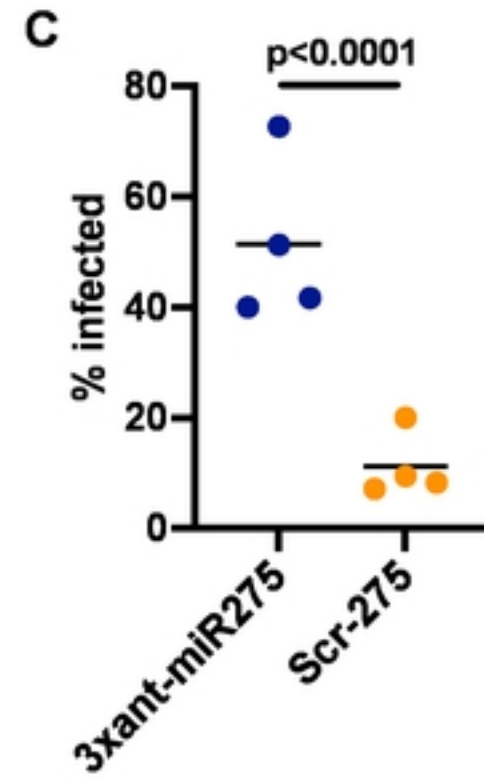
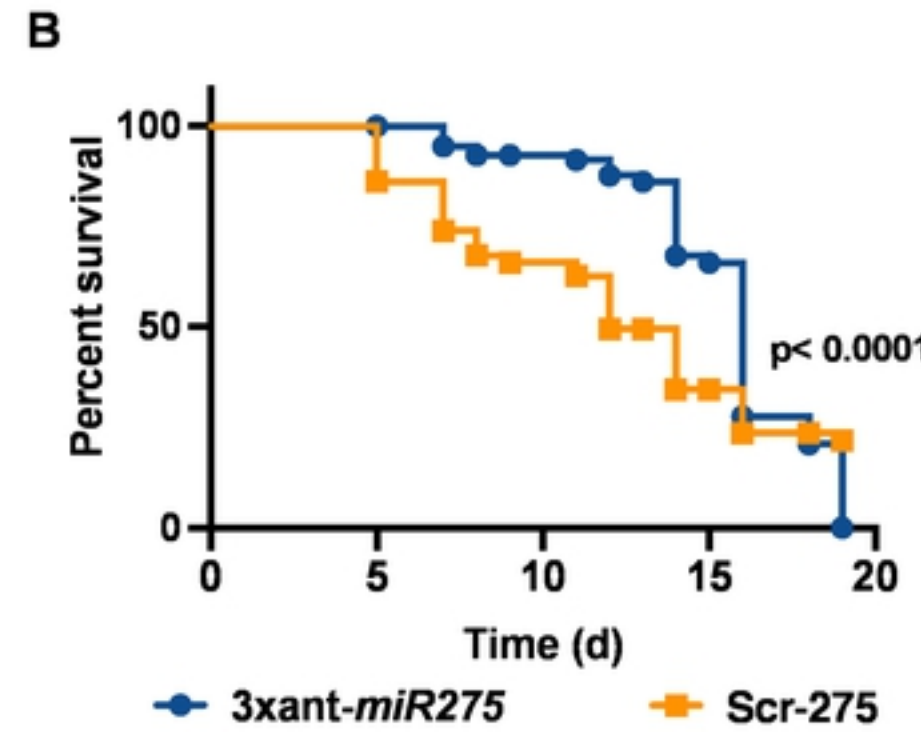
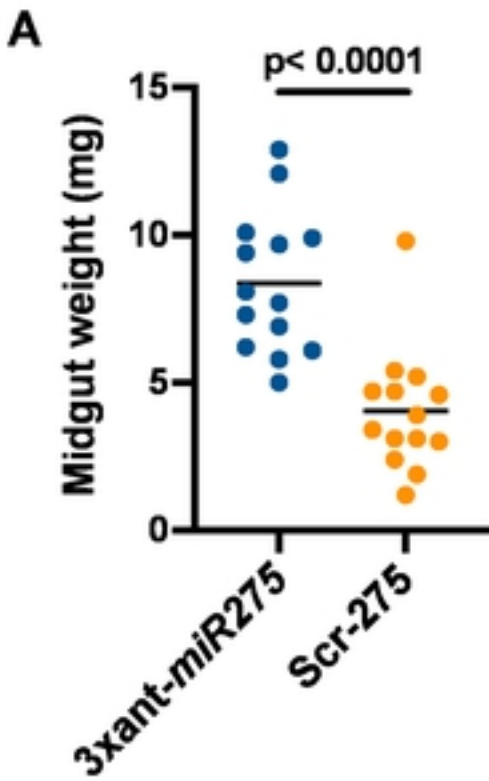
1059 **Table S2. Summary of reads mapping.**

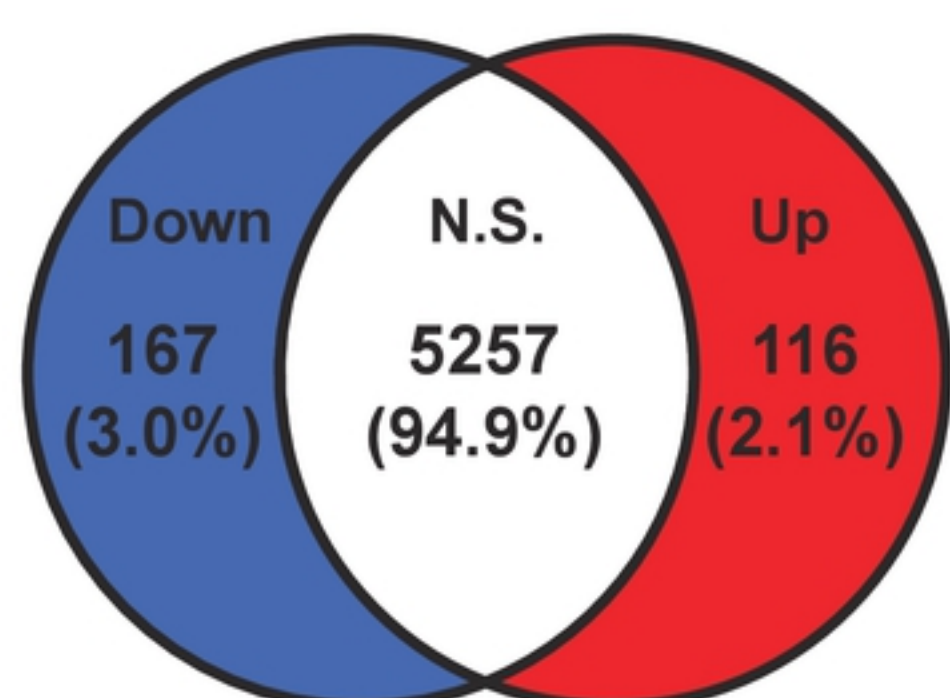
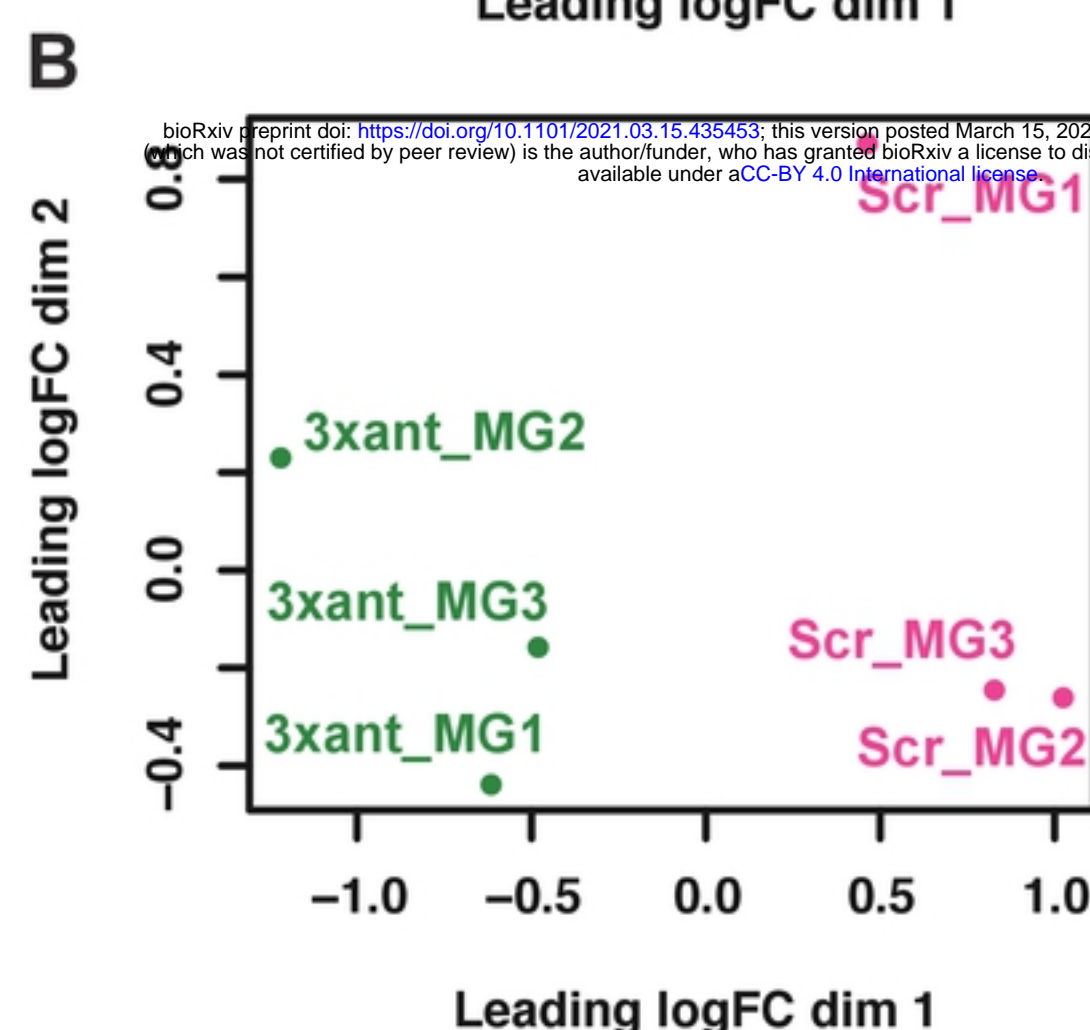
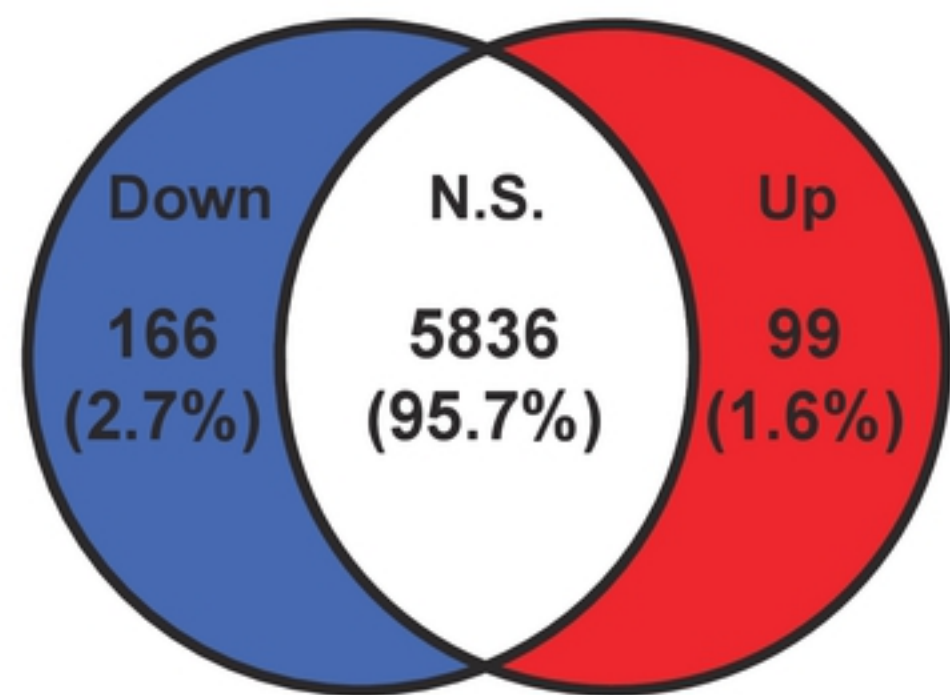
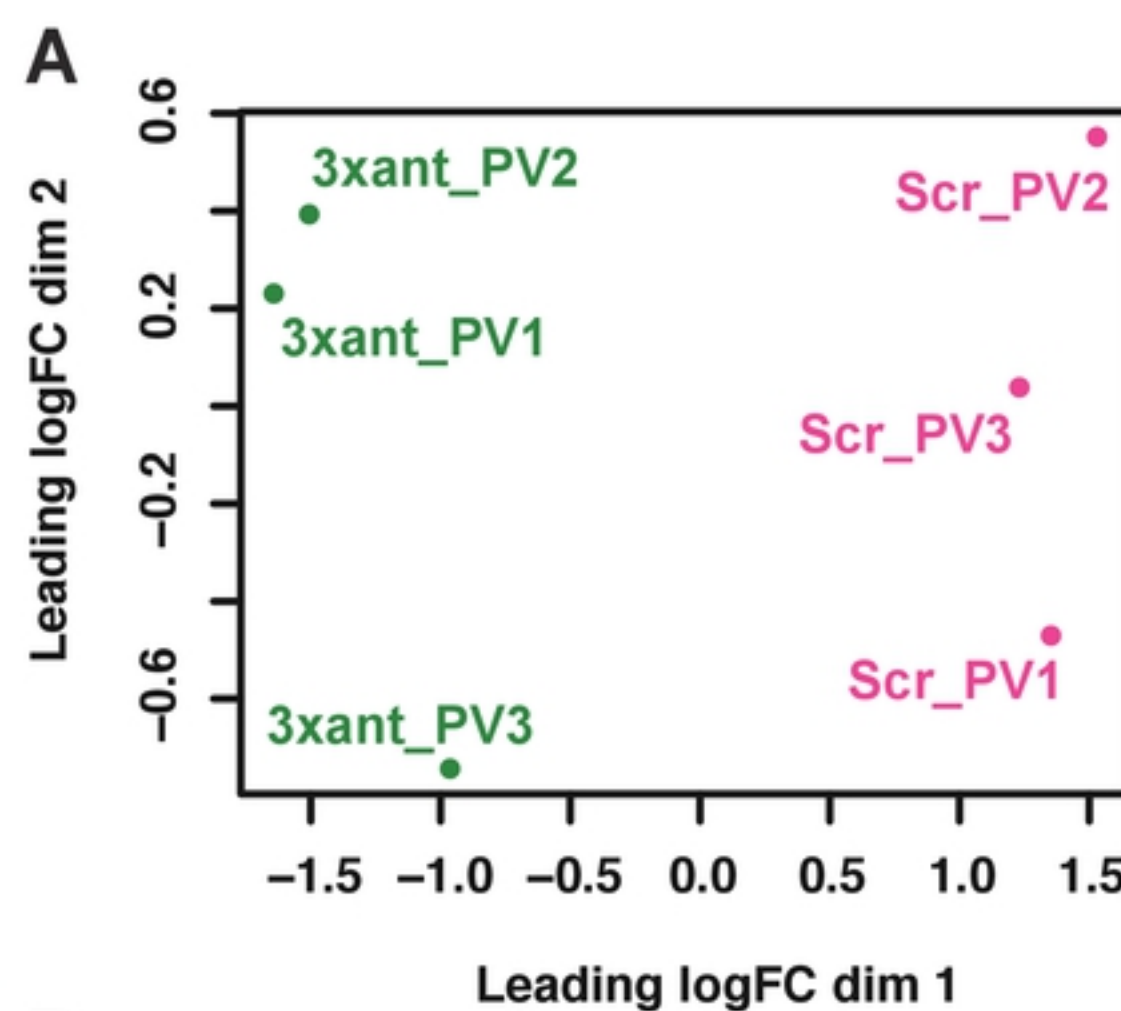
1060 **Table S3. Dataset. GO enrichment analysis.**

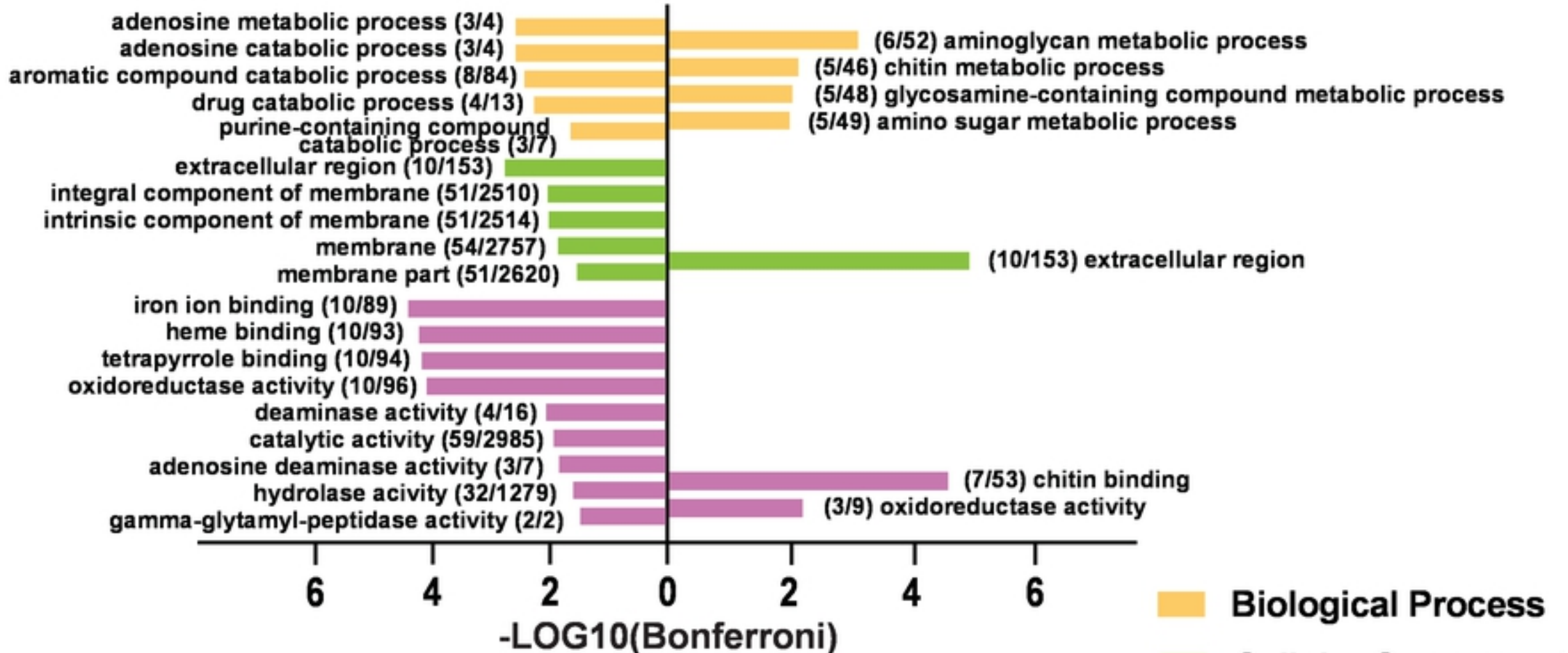
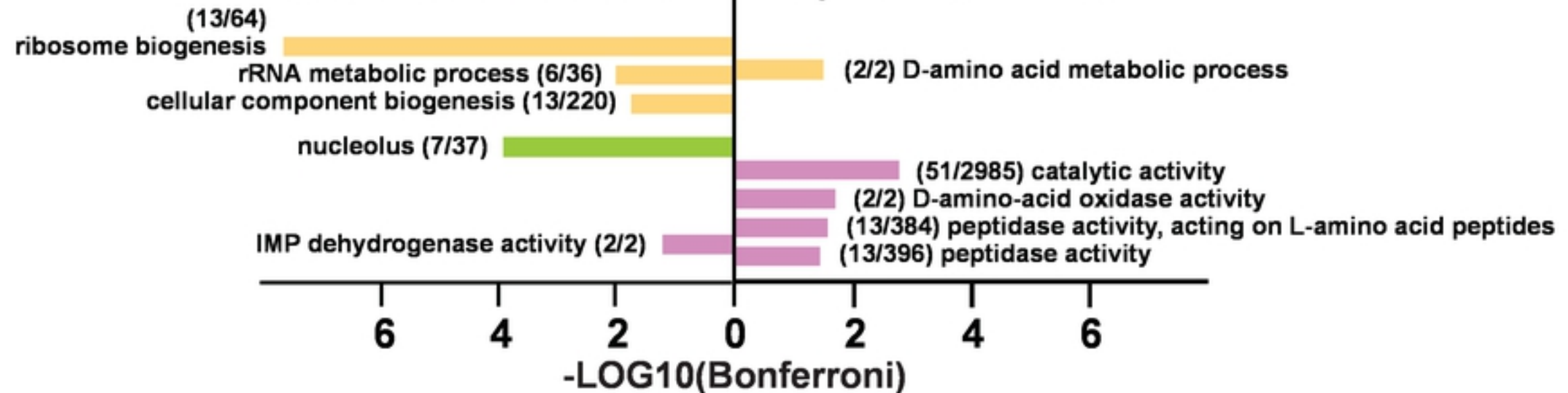
1061 **Table S4. Dataset. Raw data and DE analysis of cardia transcriptome.**

1062 **Table S5. Dataset. Raw data and DE analysis of midgut transcriptome.**

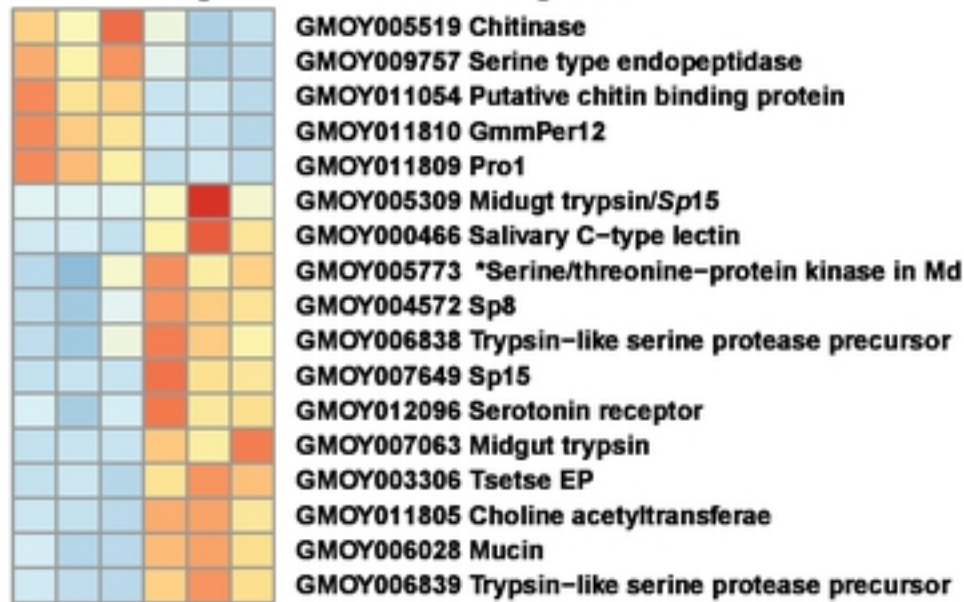




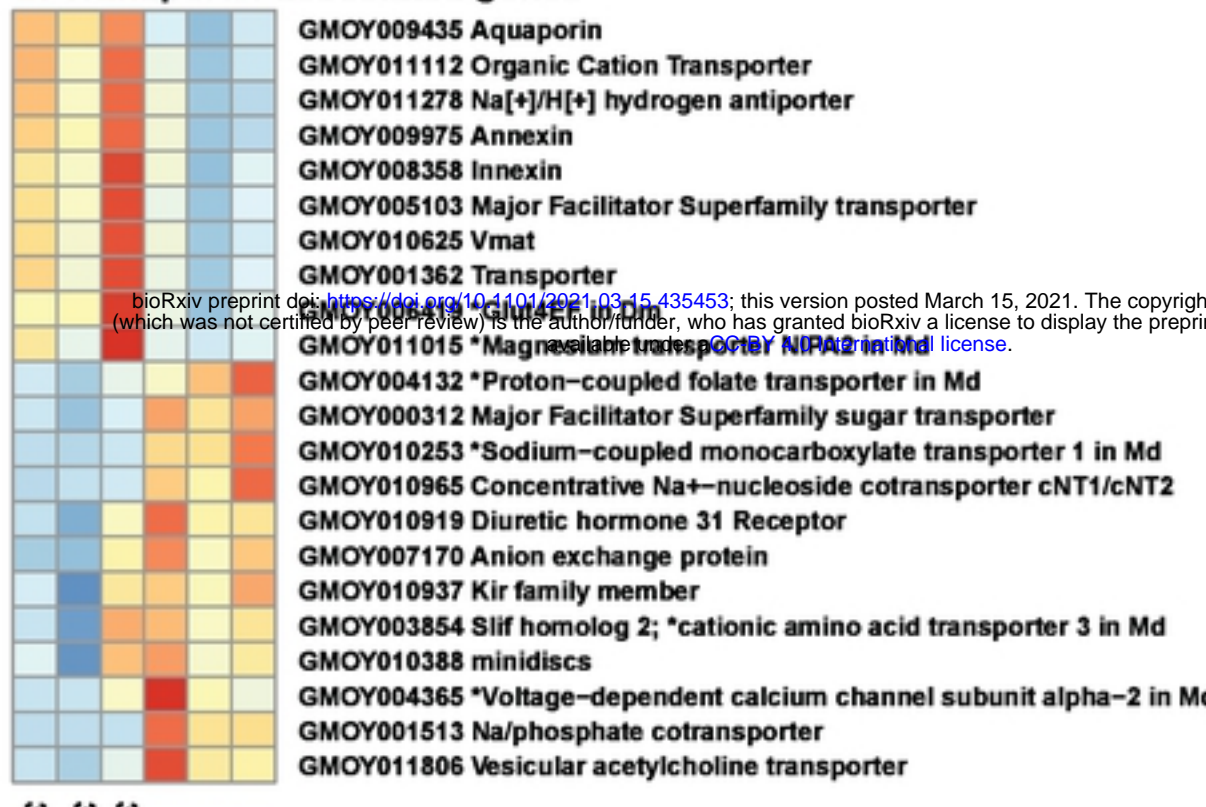


A**Down in 3xant-miR275****Up in 3xant-miR275****B****Down in 3xant-miR275****Up in 3xant-miR275**

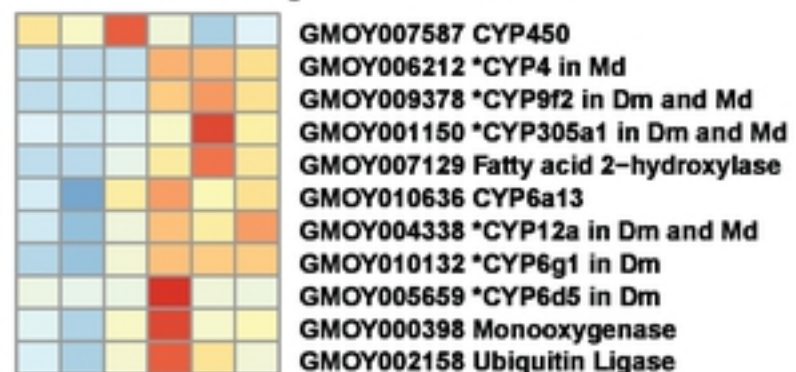
A. PM & digestion associated genes



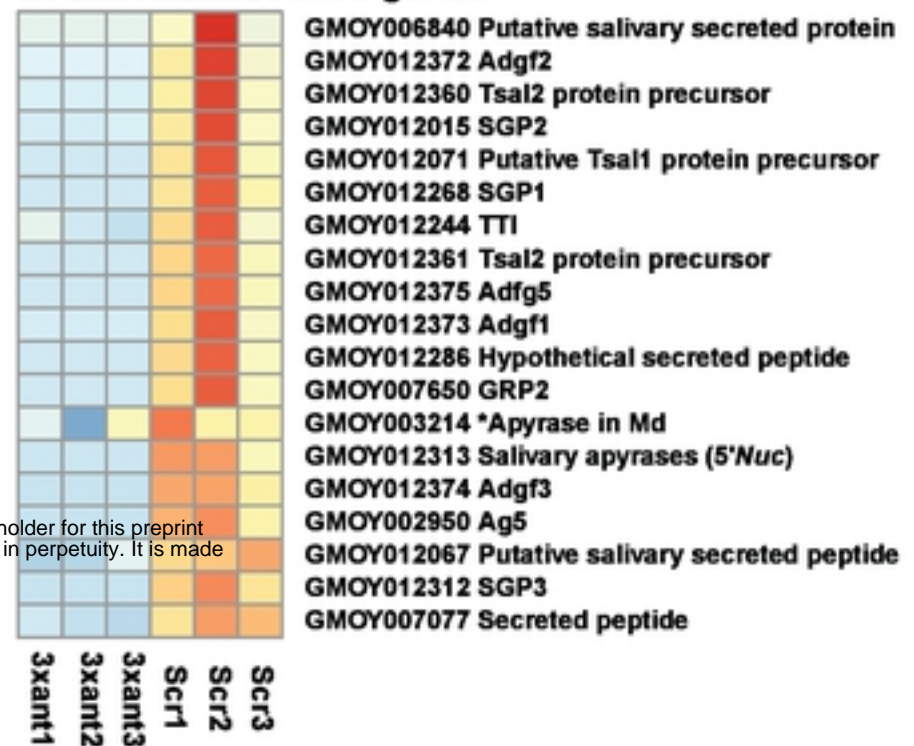
C. Transporter associated genes



B. Heme binding & detoxification



D. Saliva associated genes

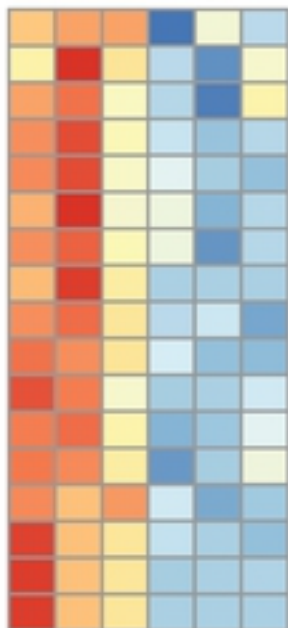


Low

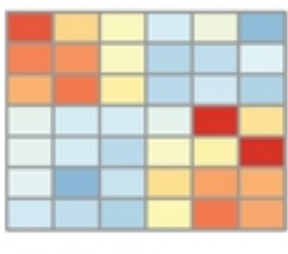
High

3xant1 3xant2 3xant3 Scr1 Scr2 Scr3

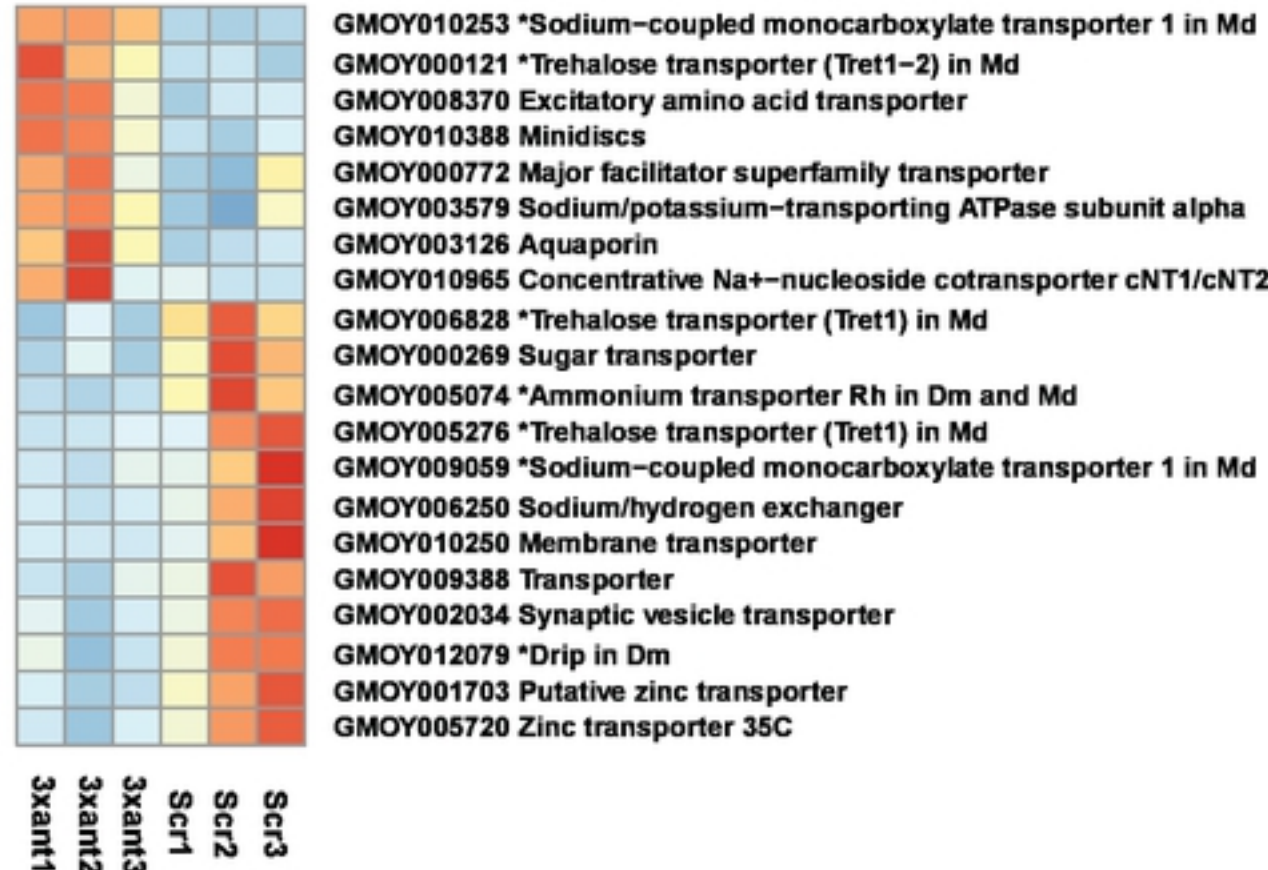
A. PM & digestion associated genes

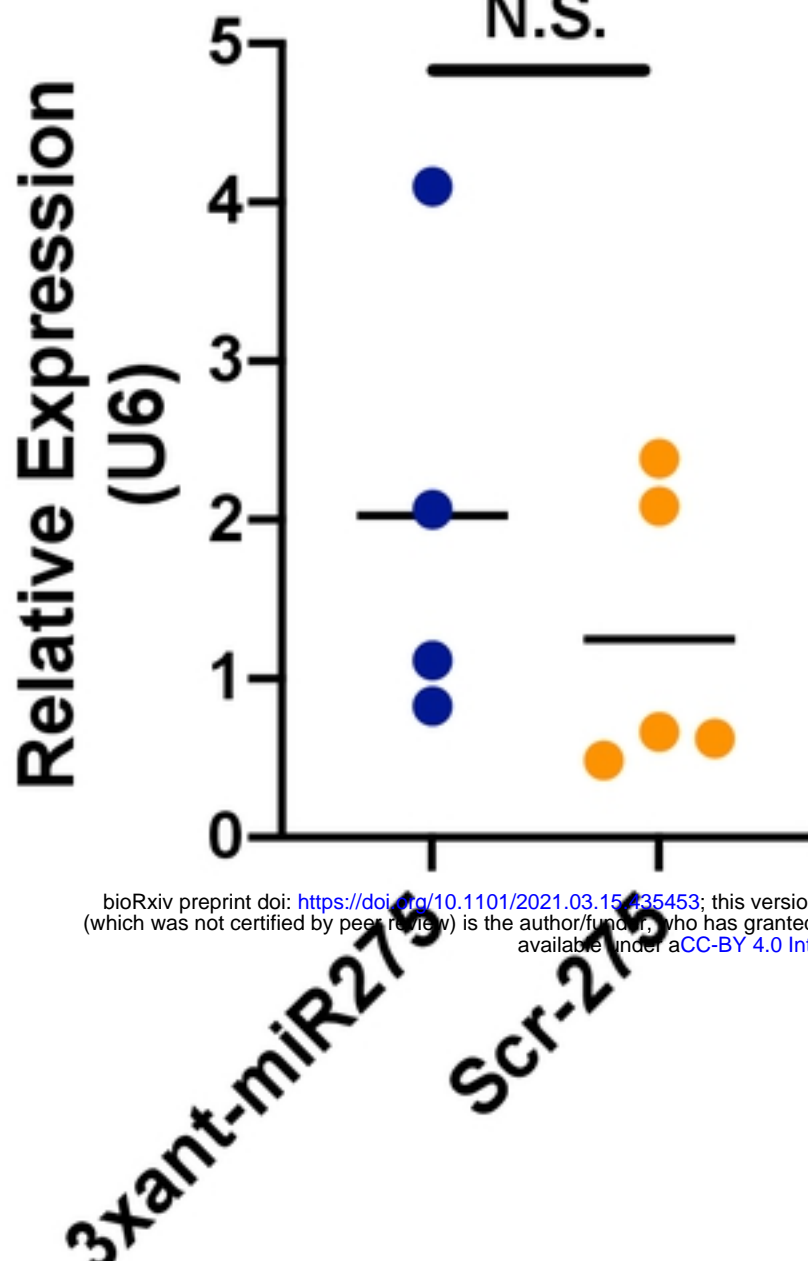
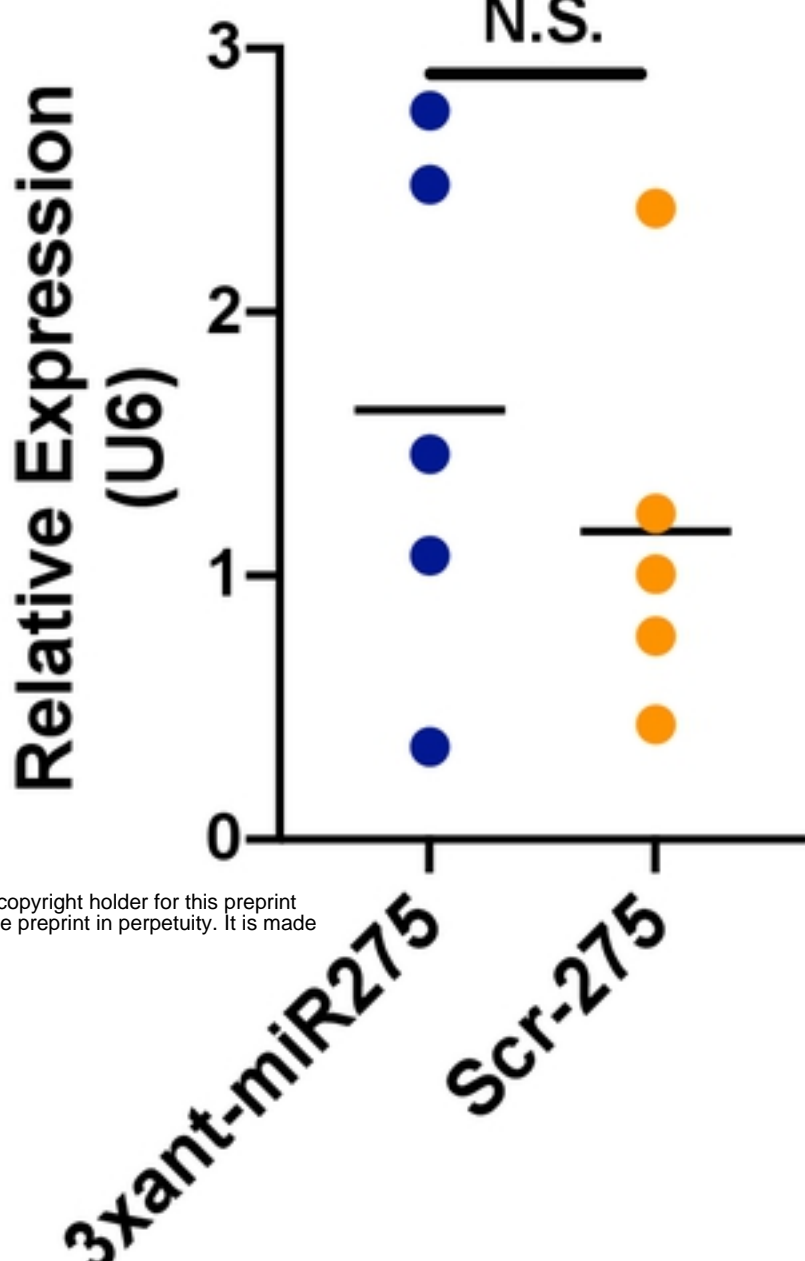
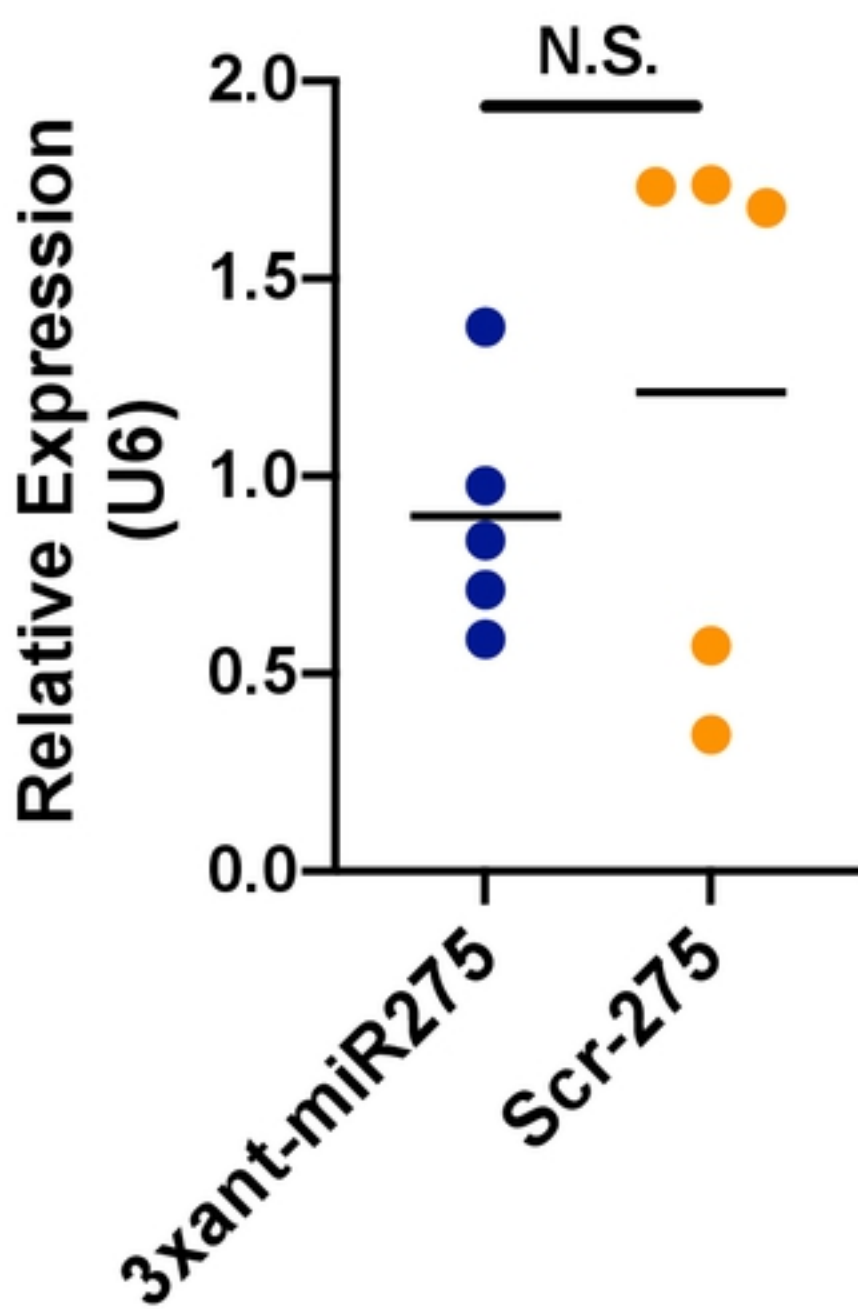
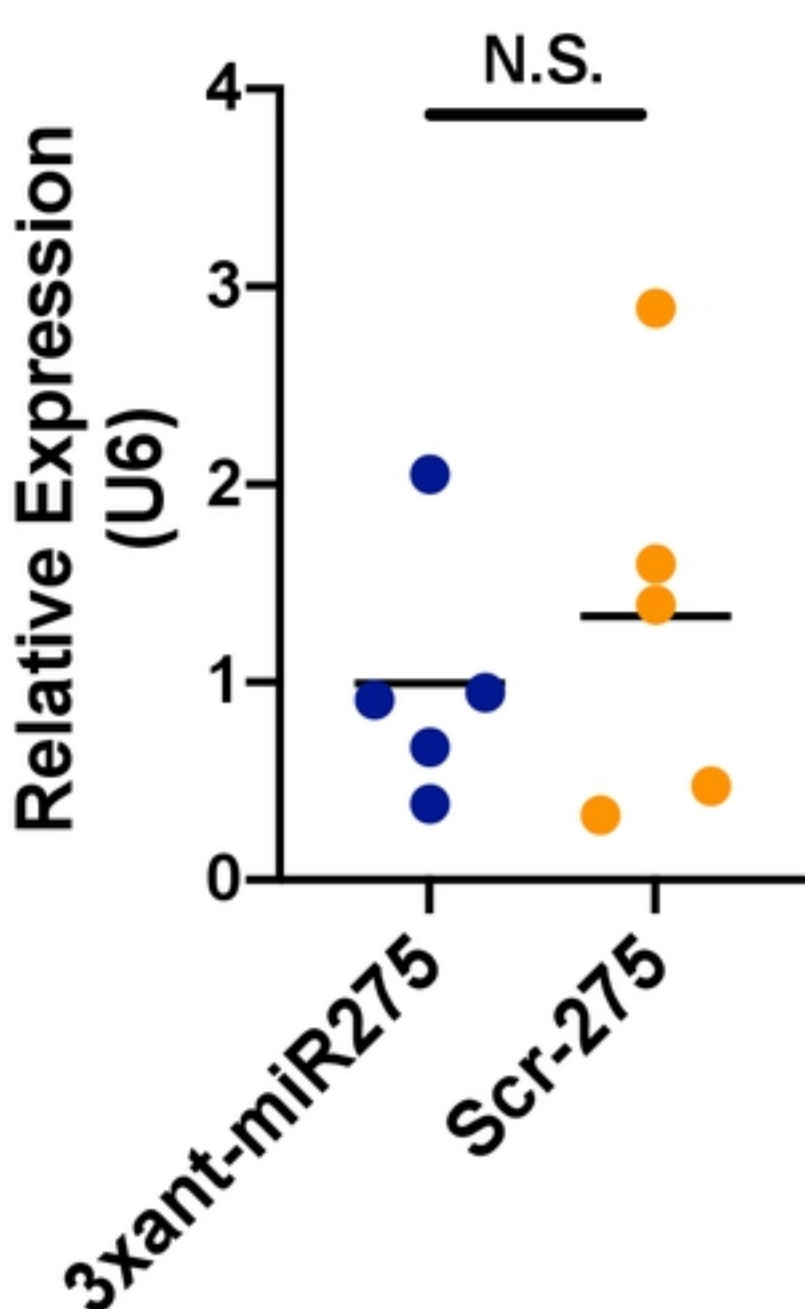


C. Heme binding & oxidative response



B. Transporter associated genes



A**miR275****B****ADGF3****C****ADGF5****D****SGP1**

bioRxiv preprint doi: <https://doi.org/10.1101/2021.03.15.435453>; this version posted March 15, 2021. The copyright holder for this preprint (which was not certified by peer review) is the author/funder, who has granted bioRxiv a license to display the preprint in perpetuity. It is made available under aCC-BY 4.0 International license.